Report SDSMT/IAS/R-92/03 May 1992

# T-28 PARTICIPATION IN THE COOPERATIVE OKLAHOMA PROFILER STUDIES (COPS-91)

By: Andrew G. Detwiler and Paul L. Smith

Prepared for:
Division of Atmospheric Sciences
National Science Foundation
1800 G Street, N.W.
Washington, DC 20550

Cooperative Agreement No. ATM-9104474

Institute of Atmospheric Sciences

South Dakota School of Mines and Technology

501 East St. Joseph Street

Rapid City, South Dakota 57701-3995

## TABLE OF CONTENTS

## LIST OF FIGURES



## LIST OF TABLES

# 1. INTRODUCTION

The armored T-28 research aircraft participated in COPS-91 (Cooperative Oklahoma Profiler Studies) at the request of Prof. Kultegin Aydin of The Pennsylvania State University. COPS-91 was designed to determine the value of a wind profiler network deployed over a portion of the central Great Plains for detecting the sub-synoptic-scale circulations and forcing for vertical motions associated with various severe storm phenomena. As it turned out, the profiler network was not completely operational during the April - June 1991 COPS-91 experiment. However, detailed observations of several mesoscale convective systems (MCS), squall lines, and other severe storm phenomena were made using a National Oceanic and Atmospheric Administration (NOAA) WP-3 aircraft with an airborne Doppler radar, coordinated mobile radiosonde launches (including electrical as well as standard meteorological measurements), a surface mesonet, the National Severe Storms Laboratory (NSSL) Cimarron radar, and other observing systems.

Professor Aydin's goal was to obtain multi-parameter data from the Cimarron radar and use *in-situ* aircraft microphysical data to verify micro-physical retrievals based on the radar data. He requested the T-28 flight support to acquire the needed microphysical observations. The T-28 was also able to supply data of use to storm dynamicists and electrical researchers involved in COPS-91, since the regions of the storms of most interest to Aydin were also of great interest to them. For its last flight of the COPS-91 program, the T-28 was used in the unusual (for it) role of measuring turbulent fluxes of heat through the boundary layer for comparison to surface-based microwave wind profiler data.

Allocation of the T-28 to support COPS-91 was recommended by the National Science Foundation (NSF) Observing Facilities Advisory Panel at its 1990 fall meeting. Field operations were funded through the NSF Division of Atmospheric Sciences facilities deployment pool.

The aircraft and supporting staff were based at Norman, Oklahoma during the May-June 1991 period of field operations. Appendix A summarizes the instrumentation complement carried by the aircraft during the project. The aircraft was directed by radio from the NSSL facility at Norman, using for guidance radar data remoted in from Cimarron, radar flight track information received via phone line from the Federal Aviation Administration (FAA), and Global Positioning System (GPS) flight tracks and meteorological data telemetered from the aircraft. This was the first T-28 field project on which the new digital data telemetry system and the GPS system were available for use. There were nine research flights, including

the boundary layer flight (during which there were no cloud penetrations). Together with the ferry and test time, this resulted in utilizing 32 of the 40 flight hours allocated.

Table 1 gives a summary of all the T-28 flights during COPS-91. Table 2 provides capsule summaries of the nine research flights. In general, better and more extensive multiparameter radar data were acquired as the project progressed, making data from the June flights the most important for comparison to radar observations. A large hailstorm complex was studied on the 5 June flight. There were two flights involving long traverses through stratiform regions behind decaying storms, and the remainder of the flights involved penetrations of smaller thunderstorms. Good coordination between ground-launched electric-field-mill balloon packages and T-28 and WP-3 airborne field mill measurements was achieved on 2 June in stratiform clouds.

The purpose of this report is to provide an initial survey of T-28 data gathered during this project. Section 2 contains a daily accounting of

**TABLE 1**

T-28 Flights Supporting COPS-91

| DATE (1991) | FLIGHT | TIME (hrs) | PURPOSE |
|---|---|---|---|
| 13 May | 538 | 3.2 | Ferry Rapid City to ICT |
| 14 May | 539 | 1.5 | Ferry ICT to OUN |
| 17 May | 540 | 1.7 | Test |
| 19 May | 541 | 2.1 | Research |
| 21 May | 542 | 2.3 | Research |
| 23 May | - | 0.6 | Ground Test |
| 24 May | 543 | 2.6 | Research |
| 30 May | 544 | 2.8 | Research |
| 01 Jun | 545 | 2.2 | Research |
| 02 Jun | 546 | 1.4 | Research |
| 05 Jun | 547 | 2.5 | Research |
| 08 Jun | 548 | 2.1 | Research |
| 11 Jun | 549 | 2.9 | Research |
| 12 Jun | 550 | 1.7 | Ferry OUN to HYS |
| 12 Jun | 551 | 2.1 | Ferry HYS to Rapid City |
| Total Hours: | 31.7 | | |

**TABLE 2**

Brief Summary of T-28 Research Flights During COPS-91

| | | |
|---|---|---|
| 19 May | - | attempt to coordinate with balloon-borne electric field mill launch on storm to west of Cimarron radar. |
| 21 May | - | coordinate with multi-parameter radar on storm to west of Cimarron, then investigate electrical aspects of another storm well to the east. |
| 24 May | - | coordinate with multi-parameter radar on storms to east of Cimarron. |
| 30 May | - | coordinate with multi-parameter radar on storms to west of Cimarron. |
| 1 June | - | coordinate with multi-parameter radar on storms to west of Cimarron. |
| 2 June | - | coordinate with electric field balloon launches and multiparameter radar on line of rain cells to southwest of Cimarron. |
| 5 June | - | coordinate with multiparameter radar on hailstorm just northeast of Norman. |
| 8 June | - | coordinate with multiparameter radar on long flight through stratiform debris south of Cimarron. Clouds fell apart before a balloon-borne field mill launch could be executed. |
| 11 June | - | low-level clear-air overflights of wind profilers at Amber and Purcell. |

T-28-related activities. Section 3 gives a statistical description of all the cloud penetrations. Section 4 describes data analyses underway as of the date of this report. Further reference material is given in the four appendices.

## 2. SUMMARY OF DAILY ACTIVITIES

The T-28 facility staff for this project included:

Dan Custis - pilot
Jon Leigh - mechanic
Gary Johnson - engineer
Ken Hartman - programmer
Dennis Musil - scientist/meteorologist
Andy Detwiler - facility scientist

A chronological account covering the major T-28 activities during the project follows. Flight times shown are takeoff and landing times (all CDT).

Monday, 13 May: Custis left Rapid City about 0930 MDT and ferried the T-28 to Wichita, Kansas. There he was interviewed by a reporter for the Wichita Eagle. The story, along with a color photograph, appeared on the front page the following day.

Tuesday, 14 May: Custis ferried the T-28 from Wichita to Westheimer Field in Norman, Oklahoma. He arrived around noon. The rest of the staff arrived later in the afternoon.

Wednesday, 15 May: The telemetry receiver and communications radio, both in the NSSL COPS operations room, were connected to antennae on NSSL roof. Telemetry between NSSL and T-28 parked on apron in front of Aeroflite main hangar was tested and found to be working well.

Friday, 17 May: The T-28 made a test flight for system check purposes.

**Flight 540**
17:46 - 19:00 CDT

The flight was to the southwest, getting out more than 100 km from Westheimer Field. Data were only recorded for the period 181232-190641. There were no cloud penetrations except when passing through a shallow deck at the top of the boundary layer just prior to landing. These clouds were warm and contained no precipitation. The telemetry link was lost for large parts of the flight; when the link was re-established, data transmission picked up where it left off. Swapping the leads to the antennae for the radio and the telemetry receiver degraded radio communications and only marginally improved telemetry.

The RATS (system for transmitting aircraft position information from FAA radar at Tinker Air Force Base to NSSL) tracking display worked. The transponder code was changed several times during the flight despite prior arrangements with FAA to keep a fixed code for the entire project. This made tracking more complicated as the display program had to be told to look for different codes as the T-28 code was switched.

The accelerometer vertical-acceleration signal did not record and the 2D-P probe had a malfunction. Some noise showed up in the static pressure, similar to what has been seen in the past. Also, there was some noise in the temperatures - larger amplitude in the Rosemount than in the reverse-flow temperature (RFT) data. (This noise could have been due to radio interference.)

Saturday, 18 May: The 2D-P "measles" (speckled bits) were fixed for the most part and the 0.002-second-duration empty buffers eliminated.

Sunday, 19 May: The T-28 investigated some short-lived rain cells, first to the east and then to the west of Norman.

**Flight 541**
16:18 - 18:00

Two penetrations were logged in the eastern clouds at 5 km MSL altitude and four in the western ones at altitudes ranging from 4.5 to 3.3 km. An attempt was made to coordinate the penetrations of the western clouds with a ground launch of a balloon-borne electric-field-mill package. T-28 penetrations caught the cloud in its mature stage, but the balloon van was delayed by traffic and launched into the debris of the cloud about 25 min after the T-28 left. Vertical electric fields reported by the T-28 near the mature stages of these short-lived clouds were a few tens of kilovolts per meter and similar to those found by the balloon-borne field meters in the debris about one-half hour later. The pilot reported supercooled rain.

The Cimarron dual-polarization signal processing was not working. The T-28 air traffic control (ATC) transponder appeared to be intermittent. The telemetry system was successful in sending data at only about half real-time, so the telemetry data being received as the plane landed was from just after takeoff almost an hour earlier! The reverse-flow temperature showed some noise on the third penetration that might have been due to shedding ice. No other

major instrumentation problems were noted. The GPS location system worked well, although position was lost intermittently, most often during turns.

Accelerometer data were not recorded. An attempt to differentiate rate of climb to obtain the vertical acceleration term in updraft computation proved unsatisfactory.

Tuesday, 21 May: The ATC transponder was found to have a loose wire. The ground telemetry-system setup was changed so that the receiver was in a penthouse on the roof of NSSL lab, leaving only a short (~10 m) lead from the antenna to the receiver.

Weak moist southerly flow across the state due to a subtropical depression along the Texas coast set up conditions for a loosely-organized cluster of thunderstorms in the Norman area.

**Flight 542**
15:35 - 17:35

Three penetrations were performed on collapsing storms to the west of Norman. The aircraft was then brought to the east of Norman and made two penetrations on storms building there. These storms were beyond range for radar ZDR, but were of interest electrically.

The pilot had been throttling back if storms were not too severe, leading to extended flight durations. Typical true airspeeds ranged between 80 and 90 m $s^{-1}$. Due to the relatively low altitudes, mostly around the freezing level, he had also been opening the canopy to cool the cockpit. This did not appear to influence any of our research instrumentation.

Telemetry data reception terminated completely on takeoff, although the indicator lights on the receiver indicated that the signal was still being detected. This led to investigation of the link between the data system and telemetry transmitter on the aircraft, which operates through the print spooler buffer attached to the data acquisition computer.

The GPS track was generally good. There were a few spots later in the flight where sufficient data were not available for a reliable track.

The highest precipitation particle concentrations occurred on the final penetration, as evidenced by both the 2D-P and the foil impactor.

Particles large enough to trigger the hail spectrometer were encountered on the last penetration, which was done visually through a growing tower.

Only weak electric fields were encountered during the penetrations on the storm to the west. Predominantly positive vertical fields with peak magnitude of 40 kV/m were encountered on the first penetration to the east, while a strong positive, then negative, field couplet reaching from +20 to -30 kV/m was encountered on the final penetration. (There was likely a strong along-fuselage field component contaminating the vertical field measurement during this penetration; this couplet of positive and negative field probably signifies passage through the central region of a charge center at the aircraft altitude.)

There were no significant measurement problems during the flight. For the first time during COPS-91, the Cimarron radar ZDR signal was available.

Wednesday, 22 May: Rewiring the connections between the data acquisition system, the printer buffer, and the telemetry transmitter on the aircraft put the buffer under hardware rather than software control. This eliminated the possibility of the buffer going into a wait-state if it receives a "CTRL-S" pattern, which then may lead to a failure to hand data on to the telemetry system.

Thursday, 23 May: The cable between the data acquisition computer and the telemetry serial box was seated more firmly. Also, the accelerometer was fixed.

Friday, 24 May: The Norman area continued to be in moist southerly tropical flow due to a depression in the Gulf of Mexico. There were many outflow boundaries in the region from MCS and large-storm activity overnight.

**Flight 543**
15:25 - 17:35

The T-28 headed for a complex of storms east of the Cimmarron radar. They were slow-moving and not severe, but very wet. Eleven penetrations can be distinguished, although the aircraft stayed in-cloud most of the time. (The pilot lumped the last four penetrations into two.) Rain accumulations of 4 inches/hour were reported from parts of this slow-moving storm complex, leading to flash flooding.

Good coordination between the Cimarron radar and the T-28 was obtained. High-reflectivity regions were repeatedly penetrated at altitudes between 4.5 and 2.5 km MSL (about -5 to +10°C).

Penetration data showed the storms to be composed of a multitude of small convective cores with diameters of a kilometer or two. There was one region extending over 10 km where these convective elements were combined into a broad updraft region with peak updrafts exceeding 10 m $s^{-1}$ at the freezing level. Echo tops exceeded 13 km in this region.

High concentrations of graupel and raindrops were found. A few particles exceeded 5 mm in diameter, but none exceeded ~8 mm diameter. The pilot reported frequent lightning and updrafts/ downdrafts reaching 1500 ft/min.

The 2D-P and FSSP probes apparently malfunctioned every time the aircraft descended to a lower, warmer altitude. This may be due to condensation on the probe optics or circuitry. The P-probe recovered after a few minutes at the new altitude. The FSSP liquid water concentrations appeared to be too low for most of the rest of the flight following the first descent.

On the first descent from the -5° to the 0°C level, the hail spectrometer output showed high concentrations of particles reaching 4.5 cm in diameter. This was probably due to ice shedding off the aircraft or the probe itself. The presence of such large particles in such concentrations was not supported by the foil or 2D-P data, or the radar observations.

Due to the long period spent in-cloud, the foil impactor exhausted its foil supply part way through the sixth penetration, at ~16:28. The audio tape containing pilot's comments ran out during the tenth penetration at ~17:08.

RATS tracking worked very well. Modification of the software brought in new aircraft positions more frequently. Previously some good data were being rejected because they also contained extraneous characters along with the correct position. The software fix allowed these positions to be plotted on the radar display on the Sun work-station despite the extraneous characters. Coordination with the Cimarron radar worked well; precipitation particle concentrations were highest when the RATS track showed the aircraft to be penetrating the regions of strongest echo.

On landing, the baggage bay where the data acquisition computer is housed, and rear fuselage, contained much water. The cover over the telemetry antenna also contained water, that later was determined to have caused a loss of transmitted power to about 50% of the full rated power. Wetness may also be responsible for the fact that the high-voltage-discharge-wick current transducer failed to work following this flight. Despite the loss of power, the telemetry system functioned reasonably well during the flight, falling no more than ~10 min behind real time and actually being close to real time for most of the flight. Maximum flight range from Norman was ~60 km, and the telemetry worked well within 40 km. On two occasions late in the flight, the GPS lat/long values were unrealistic; the 10's digit in the lat/long was dropped (e.g., 35.28° became 5.28°).

The pilot apparently had the cockpit cracked open occasionally, even in rain. This may have added to the water accumulated in the baggage bay area.

Sunday, 26 May: The P-probe diode size in the data acquisition control table was changed from 200 $\mu$m to 187.5 $\mu$m. This is intended to coordinate the strobing of the probe so as to produce a true 1:1 x:y aspect in the images.

Wednesday, 29 May: The VOR (which had been operating intermittently) was returned to the cockpit following a couple of days in the shop; it operates reliably on the bench. The next step is to try replacing the antenna.

Differential phase information may be recoverable from Cimarron radar data.

Thursday, 30 May: A small line of small storms formed in southwestern Oklahoma around 17:00 and moved slowly towards Norman. New development on the northern end of the line came within range for multiparameter radar work.

**Flight 544**
18:24 - 20:29

Eleven penetrations were made between 19:00 and 20:00 through storms in an area ~60 mi WNW of Norman. Penetration altitudes were just above and just below the freezing level. The clouds were

A strong updraft was encountered at ~17:20 during a penetration at the freezing level; it was 5°C warmer than its surroundings. Although the computed vertical wind is only 10 m $s^{-1}$, the computation is degraded due to the fact that the pilot had to pitch down to avoid being lifted out of his altitude block. The aircraft was actually rising at ~ 25 m $s^{-1}$, which is a better indication of the true updraft strength in this case. During this penetration, the 2D-P went flaky. This behavior continued for several minutes, after which the probe recovered enough so that occasionally some good data would get through. Unfortunately, sporadic noise in the 2D-P data continued through the remainder of the flight. The 2D data during this portion of the flight will require careful editing. The current hypothesis to explain the behavior of the 2D-P is that condensation occurs in the probe or in some connector in the line from the probe to the data system when the aircraft is exposed to air that is moist and several degrees warmer than it is. No foil data are available for this period because the foil supply had been exhausted during the previous penetration (Penetration 6).

Hail spectrometer data show that larger particles generally appear on the edges of regions with high 2D-P particle concentrations. Spectrometer, 2D-P, and foil maximum sizes are in reasonable agreement. A small hailstone was found in the hail catcher upon landing. A photograph of a thin-section of this stone is shown in Fig. 1.

FSSP and J-W data are in reasonable agreement.

Pilot reports and electric field measurements on the aircraft indicated frequent lightning throughout the flight. The vertical field was generally positive through Penetration 5, when the aircraft reached ~5 km altitude. Then on later penetrations near this altitude, both positive and negative excursions were recorded. At least one electric-field-mill balloon launch went up near the location of the T-28 penetrations during the flight.

The telemetry link kept up reasonably well. The T-28 computer clock was 2 s ahead of WWV. The audio tape ran out during Penetration 9.

Upon landing, it was noted that the computer equipment area was somewhat wet again.

A succession of squall lines went over Norman later in the evening, accompanied by intense rains and high electrical activity. One balloon launch crew reported small hail.

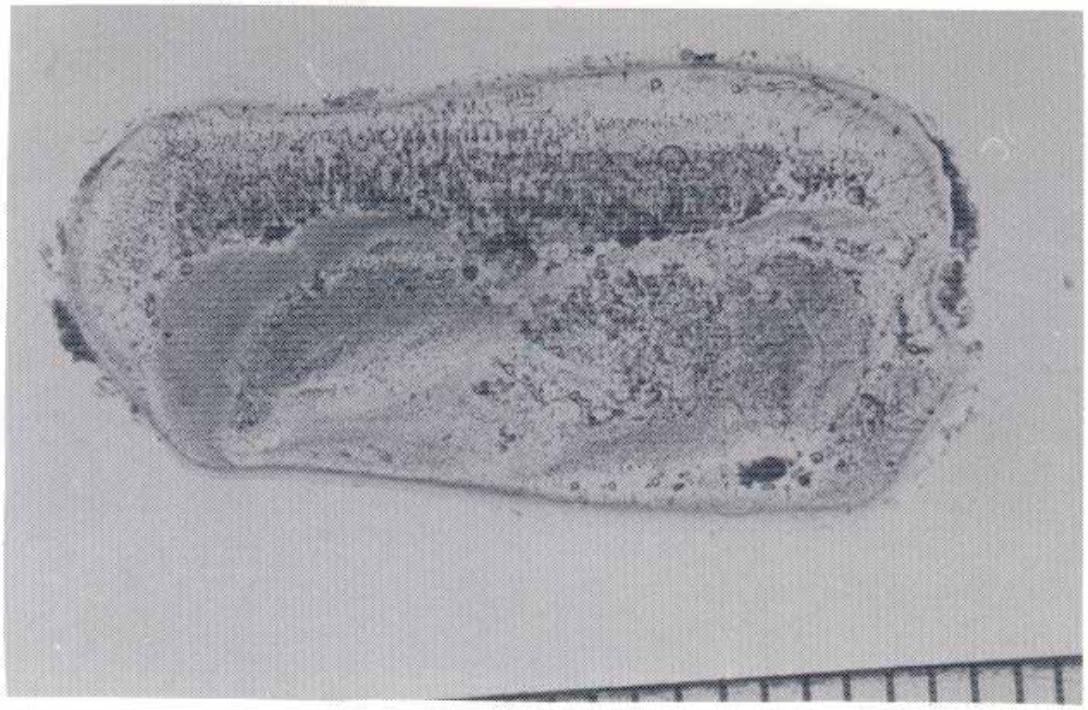

*Figure 1*: Photograph of thin-section of hailstone caught during the seventh penetration of Flight 545 on 1 June. Bubble-filled layer in upper two-thirds of photo may be water frozen onto the particle after capture. Partially-visible scale at bottom is graduated in millimeters. [Thin-section preparation and photo courtesy of Dr. Charles A. Knight, National Center for Atmospheric Research]

Sunday, 2 June: Late in the day, after it became apparent that no hail-bearing clouds were likely to develop, the T-28 launched to investigate a line of rain cells extending north-south to the southwest of Cimarron. Balloon-borne electric field mill launches were set up at either end of the line. The T-28 penetrated at about the freezing level (4.6 km) and the P-3 flew parallel tracks above at about the -10°C level (6 km).

**Flight 546**
18:21 - 19:15

The T-28 departed at 18:21, and performed one run to the south between 18:45 and 18:55. Then it returned to Norman within the next 15 minutes (re-penetrating a region slightly to the east of the first region) after developing minor engine problems. There were balloon launches at ~18:00 and 19:00 at either end of this track as well as P-3 penetrations above during this same period.

The engine problem was thought to be possibly due to an overactive alcohol pump which put too much alcohol into the carburetor during de-icing operations. This produced a change in the way the engine sounded.

The 2D-P showed aggregates during the penetration, some quite large. No particles were detected by the hail spectrometer; in light of subsequent experience, it appears the hail spectrometer was probably not functioning properly on this flight. Peak cloud water concentrations were only a few tenths of a gram per cubic meter. Vertical motions were mild, only a few meters per second at most.

The vertical electric field oscillated between -45 and +45 kV/m over distances of 10-20 km. Subsequent comparisons with balloon soundings suggest the T-28 was moving up and down through a thin charge layer that extended at least as far as the point where the aircraft turned to return home. A high proportion of positive cloud-to-ground strokes was reported from this line.

Apparent aircraft self-charging behavior was quite complex. According to the wing-tip field mills, the aircraft appeared to charge positive when approaching precipitation (and a charge region), but then the aircraft charge swung to negative when the precipitation was actually penetrated.

The pilot used the cockpit heater on descent to try to minimize condensation inside the fuselage. This seemed to work, and things were dry on landing even though the aircraft descended through rain.

The VOR and the #2 DME were inoperative during the flight.

Monday, 3 June: A comparison of flight tracks produced by the T-28 GPS system and the RATS data showed very close agreement. The latter data are only sampled every 12 seconds, as opposed to each second for GPS.

Tuesday, 4 June: A replacement VOR antenna was installed.

Wednesday, 5 June: A good hailstorm developed to the east and north of Norman by mid-morning, drifting southward. Dime-size hail was reported at Tinker AFB (north of Norman) about 10:00.

**Flight 547**
11:50 - 13:40

The T-28 made nine penetrations of very active convective cells, some containing updrafts up to 25 m $s^{-1}$. All penetrations were near the freezing level (~4.3 km MSL). The strongest updrafts were encountered on the first, fifth, and seventh penetrations. The storms were not well organized. New cells developed generally on the upwind (southwest) end of the complex, but were generally short-lived. The strongest updrafts were on the south side of the complex. Maximum reflectivities exceeded 60 dBz. The storm was most intense during the first two T-28 penetrations and then seemed to shrink, in terms of area and magnitude of maximum reflectivity, for the remainder of the flight. No stratiform anvil developed with this system.

The largest particles appeared on the first and fifth penetrations, according to a brief examination of the foil. A section of the foil from the first penetration is shown in Fig. 2. 2D-P images showed large graupel/small hail in these areas. The hail spectrometer was inoperative, but hail was audible on the windscreen mike during portions of the flight. Golfball-size hail was reported south of Norman later during the T-28 flight, but the aircraft was not in that area at the time.

The 2D-P went flaky during the second penetration in a warm updraft, but recovered and behaved itself for the subsequent penetrations. There was no evidence of wetting on either temperature probe. Cloud water measurements looked good; peak values were just over 1 g $m^{-3}$.

Balloon-borne field mills, launched into the storm complex an hour or more later than the time period of the T-28 flight, and not into the same storm the T-28 investigated, showed fields reaching 100 kV/m.

The P-3 got off around noon and stayed up for six hours. Lightning struck the P-3 and then was observed to cork-screw to the ground. The P-3 made one pass along the leading edge of the line, got bumped around quite a bit, and subsequently concentrated on the trailing edge.

The T-28 pilot reported a position directly over Tinker at 12:19:05. This should be a good spot to check RATS and GPS tracks.

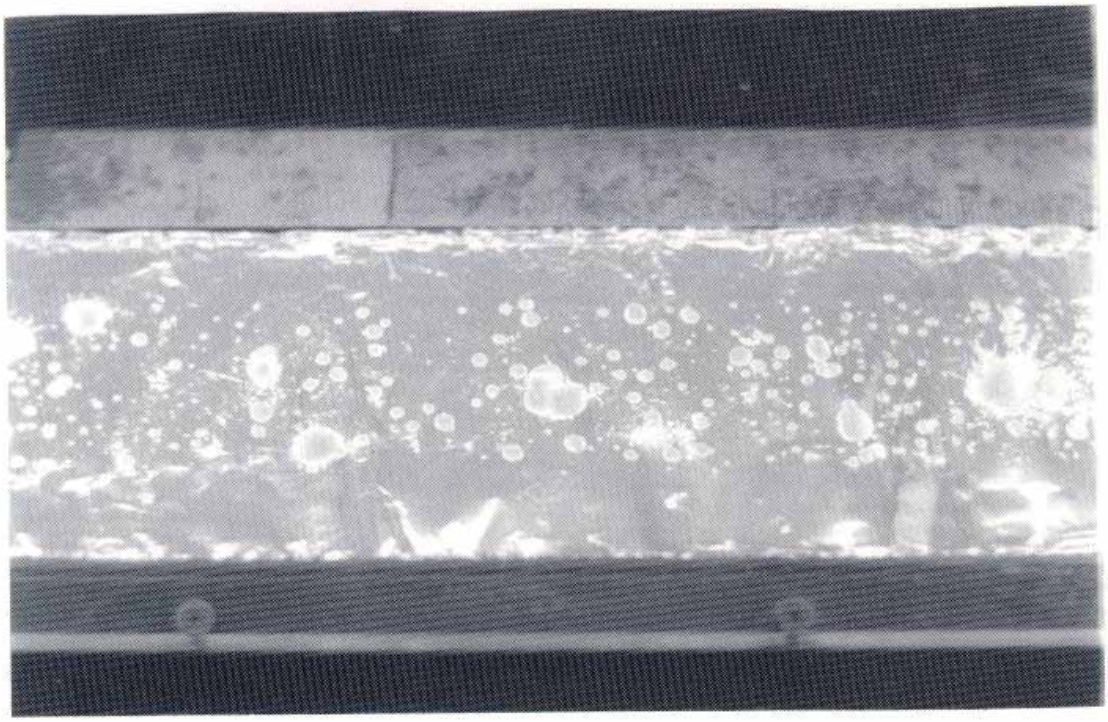

*Figure 2:* A section of foil from first penetration of Flight 547 on 5 June. Scale at top is graduated in sixteenths of inches (1.59 mm).

Saturday, 8 June: DME #2 was finally returned and re-installed in the aircraft. The VOR was also repaired and re-installed.

The T-28 crew stood by for heavy rain showers/small thunderstorms. They never got within multi-parameter radar range, so the T-28 was sent to try some penetrations along radar radials through an elevated stratiform region extending northward from a group of cells out at 90-100 km SW of Cimarron.

**Flight 548**
17:00 - 18:50

The T-28 flew south, then back north through the stratiform area, first at 5 km and then at 5.4 km MSL. The track was nearly along the 180 deg radial from Cimarron. After two circuits, the aircraft returned to base as the cloud was dissipating.

The 2D-P showed large aggregates. Maximum size indicated on the hail spectrometer was 1 cm. There were almost no impressions on the foil, indicating the particles were fragile and of low density.

There was no cloud water present according to the J-W. The FSSP showed a low cloud water concentration that was probably due to stray counts from ice particles.

Strong negative fields reaching -45 kV/m were encountered near the southern portion of the first circuit. The fields declined to no more than a few kV/m for the second circuit as the cloud layer dissipated. A field-mill-balloon launch crew reached the southern portion of the area overflown by the T-28 near the end of its flight, but decided not to launch as the clouds were visibly dissipating. A T-28 field mill self-charge test near the beginning of the flight was OK.

Telemetry started to fall behind soon after takeoff. It was more than one-half hour behind for the active part of the flight, and started to miss data after it got this far behind. It caught up again by the time of landing. The RATS track was also usually several minutes behind and sporadic through most of the flight. This made it difficult to direct the flights from the ground.

The VOR was not operating properly on takeoff, but worked OK at altitude. Some method may be needed to ventilate it.

Tuesday, 11 June: With little prospect of active storm development, some of the remaining flight hours were used to collect turbulence and related data in the boundary layer.

**Flight 549**
10:00 - 12:40

The T-28 took off for a clear-air flight over two wind profilers south and west of Norman. It flew legs at three altitudes between the profilers and perpendicular to a line between them. Dr. Richard Doviak will use the aircraft data to compute vertical heat fluxes and compare to values deduced from the profilers. He will also look at the T-28 turbulence measurements and compare to turbulence estimates derived from the profilers.

Radio noise shows up in the RFT temperature data. The VOR ventilation scheme worked well enough that the VOR was working at all but the lowest altitude (1000 ft AGL). At higher altitudes (4000 ft AGL), the telemetry was good to about 60 n mi.

The T-28 crew stood by for possible scattered thundershowers in the afternoon, but none developed close enough to the Cimarron radar for dual polarization work.

Wednesday, 12 June: Aircraft and crew departed for home.

## 3. DATA SUMMARY

The T-28 instrumentation generally performed well during COPS-91. However, some small but persistent problems should be noted by data users.

First, radio communications apparently interfered with the reverse-flow temperature signal. Pulses in the data of a few seconds duration with a nearly square wave profile should be regarded with suspicion.

Second, the 2D-P data records tend to contain noise in the first halves of buffers that corrupts the images and time bars. Although particle images can still be recognized by eye, automated image processing does not appear feasible for the first halves of buffers.

Other more intermittent problems are noted in the daily summaries in the preceding section.

COPS-91 was the first project in which the T-28 carried a GPS receiver. A comparison between aircraft position according to the FAA ATCBS radar at Tinker Air Force Base and position according to the GPS receiver is shown in Fig. 3. Published data on either system are difficult to find. Based on a series of phone calls to FAA engineers and GPS manufacturers, we compiled the tentative data shown in Table 3.

**TABLE 3**

Approximate Characteristics of GPS and FAA Secondary Radar Systems for Aircraft Location

| | GPS | FAA |
|---|---|---|
| Accuracy | ~30 m | 225 m range<br>0.25° azimuth<br>(218 m at 50 km range) |
| Resolution | ~18 m | 29 m range<br>0.088° azimuth<br>(77 m at 50 km range) |

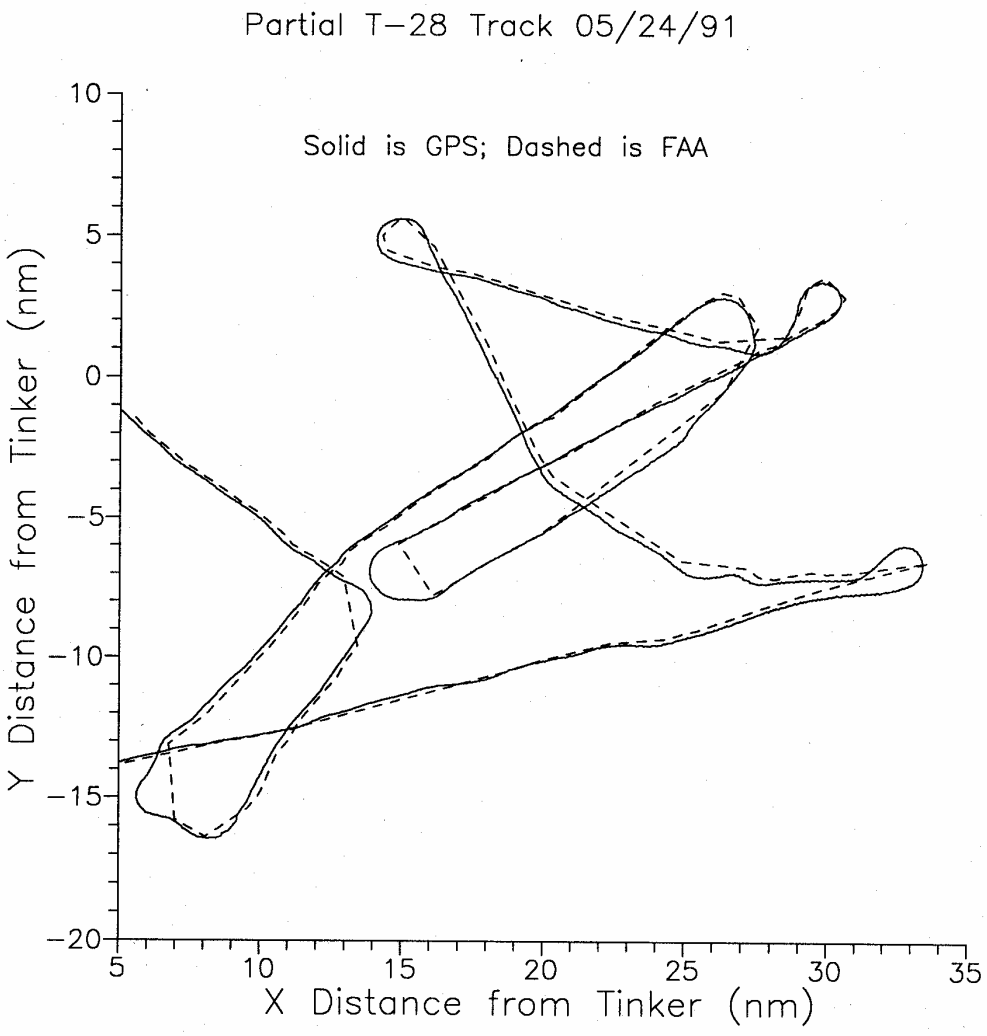


*Figure 3:* A comparison between flight tracks recorded by the FAA ATCBS radar at Tinker Air Force Base and by the on-board GPS system during Flight 543, 24 May.

The GPS performed very well during the project and appears to offer many advantages over the FAA tracking system, including better resolution, accuracy, and more timely position updates. However, the GPS data were often not available at the ground in real time due to telemetry problems, highlighting the value of redundant real-time aircraft tracking systems.

Table 4 contains a collection of summary statistics organized by segments in the flight between the times the aircraft entered and left cloud. In some cases when several small cloud elements were penetrated in quick

succession, multiple cloud episodes are lumped into one period. In some other cases, the aircraft reversed course to pass back through an interesting portion of a cloud without ever leaving the cloud. In these latter cases, a new "penetration period" is started in the middle of the reverse-course maneuver. Only rudimentary quality checks have been performed on the data at this time, so these numbers should be treated as first-look data that require further evaluation.

Appendix B lists all of the variables recorded or routinely computed from the T-28 observations, while Appendix C provides details on how each is determined. The variables tabulated here are as follows:

**Time** - time, in Central Daylight Time, 24-hour format, when the aircraft began a cloud penetration. Attempts are made to keep the aircraft data system clock set to WWV. Small deviations (plus or minus a second) may be present on any given flight.

**Dur** - duration, in seconds, of the cloud penetration.

**z** - average altitude, in geopotential meters in a standard atmosphere, during the penetration period. There may be significant differences (hundreds of meters) between this altitude and actual geometric altitude.

**T** - average temperature, in degrees Celsius, during the penetration as determined from the Rosemount aircraft temperature sensor. This sensor is subject to wetting effects and the average temperature may be biased low on many penetrations.

**LWC** - maximum 1-s value of total cloud water concentration, in $g/m^3$, as determined by the Johnson-Williams cloud water meter. This instrument has been shown to respond mainly to droplets with diameters less than 30 micrometers.

**Up/Down** - peak positive and negative vertical winds, in m/s, during the period, estimated from changes in aircraft pressure altitude computed from centered 2-s differences with some corrections applied. [See *Kopp,* 1985]

**Ez** - vertical electric field, kV/m, as determined from the T-28 electric field mills and corrected for aircraft shape effects and the roll angle of the airplane. Peak negative and positive values during the period are given. A positive vertical field component would force a positive test charge to drift upward, and is indicative of positive charge below the aircraft and/or negative charge above the aircraft.

**TABLE 4**

T-28 COPS-91 Flight Summary Statistics

| Pen Type | Time (CDT) | Dur (s) | z (m) | T (°C) | LWC (g/m$^3$) | Up (m/s) | Down (m/s) | Ez (kV/m) max- | Ez (kV/m) max+ | Ey (kV/m) max- | Ey (kV/m) max+ | Max Sh/Or Conc (1/m$^3$) | Max 2DP Conc (1/m$^3$) | Max Hail Conc (1/m$^3$) | Max 2DP Size (mm) | Max Hail Size (mm) | Hydromets |
|---|---|---|---|---|---|---|---|---|---|---|---|---|---|---|---|---|---|
| **Flt 541** | **19 May** | | | | | | | | | | | | | | | | |
| rain | 16:21:28 | 86 | 1630 | 13.0 | 0.3 | 2 | -8 | 0 | 10 | -7 | 7 | 6073 | 10068 | 4.5 | 5.6 | 45 | rn |
| small t-storm | 17:01:00 | 155 | 5090 | -6.9 | 1.6 | 16 | -13 | 0 | 27 | -6 | 14 | 19448 | 15346 | 0.2 | 16.2 | 6 | gr |
| | 17:06:14 | 165 | 5020 | -6.0 | 2.4 | 16 | -6 | -5 | 24 | -24 | 0 | 11301 | 11548 | 0 | 9.2 | 0 | gr |
| small t-storm | 17:20:30 | 230 | 4460 | -3.0 | 0.3 | 15 | -8 | -1 | 38 | -23 | 30 | 17192 | 18090 | 1.1 | 6.4 | 20 | gr |
| | 17:28:04 | 276 | 4420 | -3.2 | 0.0 | 10 | -9 | -1 | 36 | -21 | 21 | 36588 | 29922 | 0.2 | 9 | 6 | gr |
| | 17:42:02 | 88 | 3390 | 2.3 | 0.6 | 13 | -4 | -3 | 1 | -4 | 0 | 2380 | 3308 | 9.3 | 4.5 | 36 | gr |
| | 17:44:33 | 387 | 3350 | 3.2 | 0.1 | 4 | -10 | -38 | 37 | -35 | 12 | 7946 | 10333 | 3.6 | 4.9 | 17 | gr |
| **Flt 542** | **21 May** | | | | | | | | | | | | | | | | |
| dying TCu | 16:09:51 | 100 | 4280 | -0.2 | 0.3 | 3 | -10 | 0 | 1 | -1 | 0 | 7400 | 13809 | 0 | 6.2 | 0 | gr |
| | 16:12:14 | 56 | 4270 | -0.1 | 0.1 | 2 | -11 | 0 | 0 | 0 | 0 | 2510 | 6260 | 0 | 1.3 | 0 | gr |
| | 16:16:18 | 75 | 4310 | -0.9 | 0.2 | 2 | -9 | 0 | 1 | 0 | 2 | 5449 | 7987 | 0 | 4.3 | 0 | gr |
| T-storm | 17:03:00 | 70 | 4300 | 0.0 | 0.0 | 4 | -5 | -1 | 20 | -8 | 27 | 3979 | 5254 | 0 | 3.7 | 0 | gr |
| | 17:05:06 | 74 | 4260 | 0.1 | 0.1 | 6 | -5 | 0 | 5 | -4 | 2 | 8466 | 10748 | 0 | 3.2 | 0 | gr |
| | 17:09:02 | 183 | 4300 | -0.2 | 0.2 | 4 | -8 | -30 | 20 | -21 | 3 | 23701 | 14732 | 0.3 | 4.1 | 4 | gr |
| **Flt 543** | **24 May** | | | | | | | | | | | | | | | | |
| complex storm | 15:38:15 | 130 | 3880 | 0.8 | 0.0 | 15 | -9 | 0 | 19 | -6 | 9 | 10995 | 9907 | 1 | 5.8 | 6 | gr |
| | 15:47:36 | 285 | 4590 | -2.8 | 0.6 | 12 | -12 | -15 | 38 | -24 | 19 | 23818 | 31972 | 0.1 | 7.1 | 8 | gr |
| | 15:55:11 | 99 | 4630 | -3.2 | 0.1 | 10 | -8 | -59 | 22 | -21 | 19 | 13531 | 15243 | 0.8 | 6.2 | 14 | gr |
| | 16:00:25 | 230 | 3410 | 3.2 | 0.5 | 8 | -10 | -17 | 38 | -16 | 29 | 114466 | 15441 | 15.8 | 6.4 | 45 | gr,rn |
| | 16:08:31 | 113 | 3400 | 3.3 | 0.1 | 12 | -16 | 0 | 11 | -7 | 1 | 7140 | 9028 | 2.2 | 5.6 | 29 | gr,rn |
| | 16:14:09 | 435 | 3400 | 3.1 | 0.5 | 17 | -18 | -7 | 31 | -16 | 13 | 85603 | 53783 | 1.3 | 10.6 | 20 | gr,rn |
| | 16:25:00 | 90 | 2550 | 9.1 | 0.8 | 11 | -11 | 0 | 5 | -1 | 1 | 80401 | 229 | 0.1 | 5 | 4 | gr,rn |
| | 16:28:00 | 501 | 2460 | 9.3 | 0.6 | 12 | -9 | -8 | 22 | -11 | 8 | 57279 | 16315 | 0.7 | 8.8 | 45 | gr,rn |
| | 16:38:30 | 243 | 2430 | 9.5 | 0.5 | 8 | -10 | -4 | 11 | -2 | 12 | 16360 | 8729 | 0 | 6.2 | 0 | gr,rn |
| | 16:45:30 | 400 | 2440 | 8.8 | 0.1 | 10 | -15 | -12 | 24 | -6 | 13 | 68294 | 25565 | 0.8 | 12.2 | 20 | gr,rn |
| | 16:55:05 | 225 | 2480 | 8.5 | 0.3 | 13 | -8 | -8 | 19 | -11 | 15 | 10404 | 17238 | 0 | 14.2 | 0 | gr,rn |
| | 17:07:50 | 180 | 4400 | -3.2 | 0.7 | 23 | -13 | -28 | 77 | -31 | 17 | 55738 | 41287 | 0 | 8.8 | 0 | gr |
| | 17:11:50 | 194 | 4300 | -2.2 | 0.1 | 8 | -8 | -71 | 27 | -20 | 24 | 26022 | 32130 | 1.3 | 6.2 | 45 | gr |
| **Flt 544** | **30 May** | | | | | | | | | | | | | | | | |
| high-base | 19:00:55 | 55 | 4730 | -2.9 | 0.4 | 5 | -4 | 0 | 14 | -7 | 5 | 800 | 973 | 6.3 | 8.8 | 12 | gr |
| towering Cu/Tstm | 19:05:50 | 57 | 4740 | -3.1 | 0.1 | 3 | -4 | 0 | 22 | -2 | 6 | 826 | 1159 | 11.8 | 10.7 | 12 | gr |
| | 19:10:28 | 117 | 4870 | -3.9 | 0.2 | 6 | -6 | 0 | 43 | -16 | 9 | 2172 | 3662 | 11 | 11.4 | 36 | gr |
| | 19:13:38 | 142 | 4870 | -3.7 | 0.4 | 8 | -8 | 0 | 56 | -25 | 19 | 6080 | 10983 | 5.2 | 9.5 | 36 | gr |
| | 19:22:42 | 148 | 3750 | 5.9 | 0.0 | 8 | -7 | 0 | 23 | -26 | 2 | 566 | 688 | 8.9 | 9.9 | 14 | gr |
| | 19:27:50 | 89 | 3760 | 5.9 | 0.0 | 4 | -5 | -1 | 7 | 0 | 18 | 397 | 214 | 7.1 | 7.5 | 14 | gr |
| | 19:35:49 | 111 | 4720 | -2.7 | 0.4 | 12 | -4 | -5 | 8 | 0 | 21 | 2016 | 519 | 3.7 | 7.6 | 9 | gr |
| | 19:45:20 | 145 | 5310 | -7.4 | 0.2 | 7 | -7 | -23 | 18 | -19 | 3 | 4708 | 3895 | 2.7 | 6 | 12 | gr |
| | 19:48:50 | 171 | 5330 | -8.0 | 0.3 | 8 | -9 | -8 | 9 | 0 | 22 | 7829 | 7333 | 5.9 | 7.3 | 20 | gr |
| | 19:53:55 | 75 | 5320 | -8.0 | 0.2 | 12 | -7 | -4 | 32 | -23 | 0 | 8011 | 7065 | 14.1 | 8.8 | 17 | gr |
| | 20:03:24 | 199 | 4570 | -1.4 | 0.2 | 11 | -4 | 0 | 15 | -1 | 12 | 1502 | 1438 | 9.2 | 8 | 36 | gr |

**TABLE 4** (Continued)

Flight Summary Statistics

| Pen Type | Time (CDT) | Dur(s) | z(m) | T(C) | LWC ($g/m^3$) | Up (m/s) | Down (m/s) | Ez (kV/m) max- | Ez (kV/m) max+ | Ey (kV/m) max- | Ey (kV/m) max+ | Max Sh/Or Conc ($1/m^3$) | Max 2DP Conc ($1/m^3$) | Max Hail Conc ($1/m^3$) | Max 2DP Size (mm) | Max Hail Size (mm) | Hydromets |
|---|---|---|---|---|---|---|---|---|---|---|---|---|---|---|---|---|---|
| **Flt 545** | **1 Jun** | | | | | | | | | | | | | | | | |
| T-storm | 16:17:32 | 207 | 2650 | 11.1 | 0.6 | 9 | -4 | -1 | 38 | -15 | 10 | 25938 | 17889 | 3.9 | 13.5 | 45 | rn |
| | 16:23:43 | 288 | 2540 | 12.0 | 0.5 | 10 | -5 | 0 | 40 | -10 | 13 | 15358 | 12748 | 0.5 | 6.5 | 14 | rn |
| | 16:36:53 | 294 | 3760 | 4.0 | 0.7 | 11 | -8 | -2 | 38 | -10 | 18 | 28695 | 19104 | 3.2 | 8.8 | 24 | gr,rn |
| | 16:44:36 | 244 | 3790 | 3.7 | 0.3 | 11 | -11 | -9 | 29 | -29 | 10 | 16496 | 11380 | 0 | 11 | 0 | gr,rn |
| | 16:57:59 | 277 | 5020 | -4.6 | 0.4 | 13 | -5 | -12 | 31 | -13 | 16 | 33935 | 19397 | 0 | 6.2 | 0 | gr |
| | 17:09:25 | 115 | 5040 | -4.6 | 0.2 | 10 | -6 | -13 | 44 | -16 | 22 | 17472 | 9308 | 0.1 | 9.2 | 29 | gr |
| | 17:18:12 | 208 | 4340 | 0.6 | 0.4 | 10 | -13 | -18 | 34 | -14 | 18 | 188579 | 9716 | 1.6 | 8.8 | 45 | gr,rn,agg |
| | 17:23:49 | 230 | 4310 | 0.9 | 0.8 | 8 | -14 | -10 | 39 | -15 | 22 | 88204 | 11542 | 0 | 7.7 | 0 | gr |
| | 17:30:38 | 182 | 4390 | 0.0 | 0.6 | 15 | -7 | -13 | 47 | -28 | 17 | 91292 | 14153 | 0 | 7.1 | 0 | gr |
| | 17:35:43 | 418 | 4360 | 0.4 | 0.5 | 9 | -13 | -22 | 31 | -13 | 24 | 82065 | 18951 | 0 | 6.4 | 0 | gr |
| **Flt 546** | **2 Jun** | | | | | | | | | | | | | | | | |
| st-form debris | 18:39:55 | 885 | 4600 | -2.6 | 0.0 | 1 | -7 | -52 | 47 | -13 | 22 | 38396 | 43626 | M | 10.5 | M | agg |
| | 18:56:30 | 710 | 4540 | -2.5 | 0.1 | 4 | -8 | -53 | 50 | -21 | 12 | 53403 | 55757 | M | 12.9 | M | agg |
| **Flt 547** | **5 Jun** | | | | | | | | | | | | | | | | |
| dvlpng H-storms | 12:05:55 | 170 | 3830 | 2.7 | 1.3 | 11 | -15 | -5 | 13 | -5 | 11 | 18265 | 11648 | M | 10.1 | M | gr |
| | 12:10:02 | 38 | 3670 | 3.6 | 0.1 | 6 | -9 | 0 | 5 | 0 | 8 | 163 | 2936 | M | 2.8 | M | gr |
| | 12:30:40 | 35 | 4240 | -1.2 | 0.3 | 6 | -8 | -1 | 0 | 0 | 0 | 1860 | 2504 | M | 2.7 | M | gr |
| | 12:31:40 | 30 | 4250 | -1.6 | 0.2 | 6 | -7 | 0 | 0 | 0 | 0 | 2165 | 2683 | M | 3.4 | M | gr |
| | 12:33:15 | 35 | 4310 | -1.2 | 0.8 | 16 | -5 | 0 | 0 | 0 | 0 | 3342 | 2541 | M | 4.7 | M | gr |
| | 12:37:55 | 182 | 4290 | -0.9 | 0.8 | 15 | -14 | -1 | 12 | -2 | 7 | 10885 | 14526 | M | 8.6 | M | gr |
| | 12:49:40 | 150 | 4380 | -1.2 | 1.5 | 22 | -9 | -27 | 30 | -6 | 4 | 6866 | 6859 | M | 5.4 | M | gr |
| | 12:54:02 | 188 | 4290 | -1.0 | 0.1 | 4 | -7 | -1 | 18 | 0 | 26 | 4474 | 6471 | M | 7.7 | M | gr |
| | 13:10:20 | 60 | 4310 | -1.4 | 0.8 | 9 | -11 | 0 | 24 | -19 | 0 | 3316 | 2918 | M | 5.2 | M | gr |
| | 13:15:22 | 64 | 4280 | -1.1 | 0.2 | 5 | -6 | 0 | 13 | 0 | 9 | 1001 | 1620 | M | 7.5 | M | gr |
| | 13:18:53 | 142 | 4290 | -1.2 | 0.1 | 3 | -6 | 0 | 33 | -18 | 0 | 1957 | 3027 | M | 9.5 | M | gr |
| **Flt 548** | **8 Jun** | | | | | | | | | | | | | | | | |
| st-form debris | 17:38:02 | 568 | 4880 | -5.7 | 0.0 | 4 | -4 | -45 | 5 | -11 | 13 | 18818 | 31196 | 1.8 | 12 | 9 | agg |
| | 17:50:30 | 543 | 5290 | -8.1 | 0.0 | 3 | -6 | -19 | 0 | -5 | 5 | 18655 | 30097 | 2.4 | 12.3 | 10 | agg |
| | 18:03:20 | 520 | 5340 | -8.7 | 0.0 | 4 | -5 | 0 | 1 | 0 | 0 | 9103 | 10064 | 3.2 | 9.4 | 9 | agg |
| | 18:15:00 | 300 | 5340 | -8.4 | 0.0 | 4 | -4 | -2 | 0 | 0 | 0 | 8980 | 11053 | 2.9 | 11.8 | 10 | agg |
| | 18:22:20 | 190 | 5300 | -8.1 | 0.0 | 2 | -10 | 0 | 0 | 0 | 0 | 5592 | 7897 | 3.2 | 15.1 | 9 | agg |

**Ey** - horizontal electric field, kV/m, as determined from the T-28 electric field mills and corrected for aircraft shape effects and the roll angle of the airplane. Peak positive and negative values observed during the period are given. The sign convention is that a positive horizontal field component would influence a positive test charge to drift to the right of the aircraft direction of motion, indicating positive charge to the left of the aircraft and/or negative charge to the right.

**Max Sh/Or Conc** - maximum precipitation particle concentration, number per cubic meter, observed during the penetration. This estimate is based on the maximum value of 1-s counts of the number of particles entering the PMS 2D-P probe sample volume, per second. This probe responds to particles larger than roughly 200 micrometers diameter. Only the edge of a particle need be in the sample volume to trip the probe. The probe sweeps out a cubic meter in about 6 s. The concentration is computed assuming all particles activating the probe are entirely within the geometric area scanned by the probe. This assumption is not strictly true and can lead to overestimates of the particle concentrations.

**Max 2DP Conc** - maximum precipitation particle concentration, number per cubic meter, computed from the 2D-P image data in a manner described in *Detwiler and Hartman* (1991). These estimates are based on periods over which the probe was active for a total of 1 s, which may involve several seconds of flight time. Artifact images are rejected and some particles partially in the field of view are reconstructed and included in the count. This approximately doubles the volume sampling rate of the probe for the largest particles compared to the volume sampling rate obtained if only images entirely within the field of view are included. These maximum concentration estimates are typically similar to the ones based on the shadow/or counts when the probe is operating properly. The peak values are somewhat dependent on the time chosen for the beginning of the penetration as the sample accumulation process for each 1-s period will involve different portions of the cloud if it is started at different times. See *Detwiler and Hartman* (1991) for more details.

**Max Hail Conc** - maximum concentration, number per cubic meter, of particles with diameters larger than ~5 mm as determined by the T-28 hail spectrometer. This is a non-imaging, one-dimensional optical array probe with a volume sampling rate ~30 times that of the 2D-P (if partial images are included in the 2D-P sample). Large liquid drops may be counted by this probe as well as snow, graupel, and hail.

**Max 2DP Size** - maximum particle size (mm) observed by the 2D-P probe during the period. Since an attempt is made to reconstruct partial images, and the maximum dimension may be in the along-flight direction, the maximum size may exceed the nominal 6 mm effective width of the 2D-P array. Attempts are made to exclude artifact images such as splashes and streakers, but the automated rejection scheme is not 100% effective. These data have been checked with one pass of visual inspection through the most-probably misclassified images, but further examination would be prudent before basing any detailed analyses on these values.

**Max Hail Size** - maximum-size particle (mm) detected by the hail spectrometer during the penetration. Timing criteria are used in an attempt to reject counts due to water streaming off the probe housing, although this has been shown to be insufficient to eliminate all artifacts from the data. The maximum measurable size is 45 mm. Values this large in the presence of rain are probably artifacts due to water streaming off the housing. Detailed examination of the measured size spectra should be done in order to further verify the maximum sizes listed here. Maximum sizes determined from this probe are typically larger than maximum sizes determined by the 2D-P due to the larger size range sampled and the higher volume sampling rate.

**Hydromets** - a qualitative description of the most common particle type observed during a penetration, based on visual inspection of a sample of the images from each penetration.

rn = raindrops
sn = snow (dendrites, columns, etc., showing little or no riming)
gr = graupel
agg = aggregates of snow crystals

Appendix D provides the recorded GPS flight track for each T-28 research flight during COPS-91.

## 4. ANALYSES IN PROGRESS

As of the time of preparation of this report, T-28 data are involved in two ongoing analyses from COPS-91. The first is a comparison between aircraft *in-situ* data and multiparameter radar signatures obtained during the 5 June flight. This work is being performed at Penn State under the guidance of Professor Aydin. The second is a comparison between electric field structures observed by the aircraft and those observed from balloons in stratiform debris clouds on 2 June. This latter work is being performed at NSSL/University of Oklahoma by Maribeth Stolzenburg and collaborators in the atmospheric electricity group.

## ACKNOWLEDGMENTS

The T-28 facility is supported by the National Science Foundation, Division of Atmospheric Sciences, and the State of South Dakota under Cooperative Agreement No. ATM-9104474. The T-28 facility staff acknowledges with gratitude the support and cooperation received from NSSL staff and COPS-91 participants. The Canadian Atmospheric Environment Service loaned the 2D-P optical array probe that provided the primary data for the multiparameter radar study. Funds for deployment were provided from the NSF Atmospheric Sciences Division facilities deployment pool under the aforementioned Cooperative Agreement. Ken Hartman carried out much of the preliminary data processing. Patricia Peterson and Joie Robinson assisted in the preparation of this report.

## REFERENCES

Detwiler, A. G., and K. R. Hartman, 1991: *IAS Method for 2D Data Analysis on PC's.* Bulletin 91-5, Institute of Atmospheric Sciences, S.D. School of Mines and Technology, Rapid City, SD. 37 pp. + appendices.

Kopp, F. J., 1985: Deduction of vertical motion in the atmosphere from aircraft measurements. *J. Atmos. Ocean Tech.,* **2**, 684-688.

# APPENDIX A

## T-28 Instrumentation

| VARIABLE | INSTRUMENT | RANGE | ACCURACY | RESOLUTION (as recorded) | NOTES |
|---|---|---|---|---|---|
| STATIC PRESSURE | ROSEMOUNT 1301-A-4B | 0-15 psi (0-103 kPa) | ±0.015 psi (±0.1kPa) | 0.0002 psi (0.002 kPa) | • Bench calibration, 3/89 |
| | ROSEMOUNT 1301-A-4B | 5-15 psi (35-103 kPa) | ±0.015 psi (±0.1kPa) | 0.0002 psi (0.002 kPa) | • Bench calibration, 3/89 |
| TOTAL TEMPERATURE | ROSEMOUNT 102AU2AP | -30 - +30°C | ±0.5°C | 0.001°C | • Platinum wire<br>• -2 sec time constant |
| | NCAR REVERSE FLOW | -30 - +30°C | ±0.5°C | 0.001°C | • Diode<br>• Several sec time constant<br>• Bench calibration, 3/89<br>• Recovery factor adjusted, 5/89 |
| CLOUD WATER AND CLOUD DROPLETS | JOHNSON-WILLIAMS LIQUID WATER CONCENTRATION | 0 - 6 g/m2 | ±20% | 0.0001 g/m3 | • Accurate if all droplets have d < 30 μm |
| | PARTICLE MEASURING SYSTEMS, INC. FORWARD SCATTERING SPECTROMETER PROBE | Size -1 < 57 μm Concentration 0 - ≥2000 droplets/ $cm^3$ | ±1 size channel in size and ±1% in concentration at -50/$cm^3$ | 1 size channel | • 15 discrete size channels spread over an adjustable range<br>• Sampling rate 300 $cm^3$/km<br>• Accuracy of computed liquid water concentration - ±20%. Depends on processing. |
| PRECIPITATION PARTICLE SIZES AND CONCENTRATIONS | WILLIAMSON FOIL IMPACTOR | 1 - 20 mm | 0.2 mm | 0.2 mm | • Sampling rate 1.4 $m^3$/km |
| | PARTICLE MEASURING SYSTEMS, INC. 2D Precip Probe | Size 200 - 6400 μm | ±200 μm | 200 μm | • Computed ice and water concentration can vary ±50% with processing technique<br>• Sampling rate: 1.66 $m^3$/km; DAS can accept ~250 particles/sec (2500/km) |
| | HAIL SPECTROMETER | Size 4.5 mm - 4.5 cm Concentration 0 - 100/$m^3$ | ±1 size class | 1 size class | • 14 size classes<br>• Sampling rate 100 $m^3$/km<br>• Alternates with particle camera |
| | NCAR PARTICLE SAMPLER | | | | • A batch sampler, primarily for hailstones<br>• Sampling rate 2.6 $m^3$/km |
| AIRCRAFT MOTION | NCAR TRUE AIRSPEED COMPUTER | 0 - 250 kts (0 - 130 m/s) | ±3 kts (±1.5 m/s) | 0.125 kt (0.07 m/s) | • True airspeed |
| | HUMPHREY SSA09-D0101-1 VERTICALLY STABILIZED ACCELEROMETER | -1 to +3 g's<br><br>pitch -50° to +50°<br>roll -50° to +50° | 0.004 g<br><br>0.2°<br>0.2° | 0.00006 g<br><br>0.002°<br>0.002° | |
| | ROSEMOUNT 1301-D-1B DYNAMIC PRESSURE | -3 to +3 psi (-20 to +20 kPa) | ±0.1% | 0.0001 psi (0.0006 kPa) | • Indicated airspeed<br>• Bench calibration, 3/89 |
| | ROSEMOUNT 1221-F-2A DYNAMIC PRESSURE | -2.5 to +2.5 psi (-18 to +18 kPa) | ±0.1% | 0.0001 psi (0.0006 kPa) | • Indicated airspeed<br>• Bench calibration, 3/89 |
| | GIANNINI 45218YE MANIFOLD PRESSURE | 0 to 50 in Hg | ±2% | 0.008 Hg (0.03 kPa) | • Used in one vertical velocity calculation<br>• Bench calibration, 3/89 |
| | BALL ENGINEERING 101A VARIOMETER | -6000 to +6000 ft/min (-30 to +3- m/sec) | ±200 ft/min (±1 m/sec) | 0.2 ft/min (0.001 m/sec) | |
| AIRCRAFT LOCATION | NARCO NAV-122 VOR | 0 - 360° | ±2° | 0.005° | |
| | CESSNA 400 DME | 0 - 100 nmi (0 - 185 km) | 0.1 nmi (185 m) | 0.002 nmi (3m) | • Maximum 2 sec to lock on and acquire range |
| | TRIMBLE TNL3000 GPS/LORAN | (global) | 30 m | 18 m | • LORAN unit not available in 1991 |
| ELECTRIC FIELD | NMIMT Model E-100 DC Electric Field Meter | - ± 200 kV/m | | 0.01 kV/m | |

NOTE: Many of these instruments do not behave as ideal instruments. The use of one measure of accuracy over the entire range of measurement is, in many cases, questionable. An accuracy representative of the most useful part of the range is given here.

## APPENDIX B

List of Variables Recorded or Routinely Computed
From T-28 Observations

Each different variable in the data stream is indexed with a unique tag number. Those used for COPS-91 are listed here.

| Tag | Variable | Remarks |
|---|---|---|
| 100 | **Time** | The T-28 data system is always set to local time, and recorded in a 24-hour format. It is maintained within a second of WWV unless otherwise noted. |
| 101 | **Dynamic Pressure 1** | |
| 102 | **Dynamic Pressure 2** | Both dynamic pressures are read from the same pitot tube line (with the inlet out on the right wing) using two different but nearly identical sensors. [hPa] |
| 103 | **Rosemount Static Pressure 1** | |
| 104 | **Rosemount Static Pressure 2** | Both static pressures are read from the same static pressure line (inlet on the rear fuselage) using two different but nearly identical sensors. [hPa] |
| 105 | **Rate of Climb** | The instantaneous rate of change of aircraft altitude, read from a standard aircraft variometer. The recorded data data are unfiltered and much noisier than the damped cockpit display. [m/s] |
| 106 | **Rosemount Temperature** | This is static temperature computed from the reading of a standard, de-iced, Rosemount aircraft total air temperature probe. It commonly suffers from wetting and reads low in clouds. [°C] |

| | | |
|---|---|---|
| 107 | **Reverse Flow Temperature** | This is static temperature computed from the reading of a thermistor placed inside a custom-design "reverse-flow" housing. It does not normally get wet in supercooled clouds, but may get wet in warm clouds or in regions of high precipitation water concentration. Apparently, ice may sometimes build up to such an extent on the housing that temperature readings are affected even though the sensor is not wetted. [°C] |
| 108 | **Manifold Pressure** | Pressure inside the engine manifold (an indicator of power being developed by the engine) is recorded from a standard aircraft engine pressure sensor. [inches of mercury] |
| 109 | **Acceleration** | Vertical acceleration is determined by a Humphrey accelerometer. [g's] |
| 110 | **Pitch** | The accelerometer also gives angle of the fuselage relative to horizontal. [deg] |
| 111 | **Roll** | Finally, the accelerometer gives angle of the wings relative to horizontal. Angle is positive for a left bank (left wing down). [deg] |
| 112 | **J.W. Liquid Water** | The J.W. probe yields concentration of water in clouds represented in droplets less than approximately 30 $\mu$m diameter. [grams per cubic meter] |
| 113 | **VOR** | The VOR gives the direction to the VORTAC (a radio direction-finding beacon used by aircraft) to which it is tuned. [deg] |
| 114 | **DME1** | This is distance to the VORTAC to which the #1 DME is tuned. [n mi] |

| | | |
|---|---|---|
| 115 | **DME2** | This is distance to the VORTAC to which the #2 DME is tuned. If they are tuned to different VORTAC's, the recorded distances from the two DME's may be used to reconstruct the aircraft flight track. [n mi] |
| 116 | **Voltage Regulator** | Research system voltage. [volts] |
| 117 | **Heading** | Indicates direction (from magnetic north) towards which the aircraft is heading. [deg] |
| 118 | **NCAR true air speed** | True airspeed as computed by an analog computer built at NCAR during the NHRE project in the 1970's to clock the 2D-C imaging probe. [m/s] |
| 121 | **Interior Temperature** | Temperature inside the data acquisition system computer in the baggage bay. If it climbs much above 32°C, one should be wary for possible data system malfunctions. [°C] |
| 123 | **HV Current** | Discharge current from a discharge wick under the rear fuselage. Failed early in 1991. [mA] |
| 130 | **Event Bits** | Bits corresponding to various events recognized by the data system, including such things as the in-cloud switch activated by the pilot when visually entering cloud, activation of the cockpit voice recorder, etc. |
| 131 | **GPS Warning Codes** | Bits corresponding to various status messages from the GPS system. |
| 140 | **FSSP size counts** | This tag contains information concerning the number of counts in each of the 15 available FSSP size channels. [number per channel per second] |
| 141 | **FSSP total counts** | The total number of droplets counted by the FSSP during a second. |

| | | |
|---|---|---|
| 142 | **FSSP average diameter** | The average diameter of all droplets recorded during a second. [$\mu$m] |
| 143 | **FSSP concentration** | The actual concentration of droplets computed from FSSP counts divided by the volume sampled in 1 s. A rudimentary correction for probe activity is made. [number per cubic centimeter] |
| 144 | **FSSP Water** | The water concentration computed from the FSSP data for a second. [grams per cubic meter] |
| 145 | **FSSP Activity** | The fraction of time the FSSP is active during the current second. |
| 146 | **PMS 2DP Shadow Or Count** | The number of times the probe was triggered out of its wait state by the passage of a new particle. [number per second] |
| 150 | **Hail size counts** | This tag contains information on the number of particles in each of the 14 hail spectrometer size channels. [number per channel per second] |
| 151 | **Slow Particle** | The number of particles rejected because they passed through the hail spectrometer too slowly (indicating they were probably water or ice shed from the probe structure rather than hydrometeors). [number per second] |
| 152 | **Hail total counts (of 150)** | Total number of particles accepted by the hail spectrometer. [number per second] |
| 153 | **Hail average diameter** | The arithmetic average diameter of all particles accepted by the hail spectrometer in the last second. [cm] |

| | | |
|---|---|---|
| 154 | **Hail concentration** | The computed concentration corresponding to all particles accepted by the hail spectrometer in the last second. [number per cubic meter] |
| 155 | **Hail Water** | The mass concentration computed from the observed particle spectrum assuming a bulk particle density of 0.9 grams per cubic centimeter. [grams per cubic meter] |
| 160 | **Top Field Mill (low res)** | The electric field indicated by the low sensitivity channel on the field mill mounted in the aircraft canopy looking up. Field mill data are recorded at 20 Hz. [kV/m] |
| 161 | **Bottom Field Mill (low res)** | The electric field indicated by the low sensitivity channel on the field mill located in the baggage bay door looking down. [kV/m] |
| 162 | **Left Field Mill (low res)** | The electric field indicated by the low sensitivity channel on the field mill mounted in the left wing tip facing outward. [kV/m] |
| 163 | **Right Field Mill (low res)** | The electric field indicated by the low sensitivity channel on the field mill mounted in the right wing tip facing outward. [kV/m] |
| 164 | **Top Field Mill (high res)** | The electric field indicated by the high sensitivity channel on the top field mill. [kV/m] |
| 165 | **Bottom Field Mill (high res)** | The electric field indicated by the high sensitivity channel on the bottom field mill. [kV/m] |
| 166 | **Left Field Mill (high res)** | The electric field indicated by the high sensitivity channel on the left field mill. [kV/m] |

| | | |
|---|---|---|
| 167 | **Right Field Mill (high res)** | The electric field indicated by the high sensitivity channel on the right field mill. [kV/m] |
| 172 | **Latitude** | Computed internally in the GPS receiver. [deg] |
| 173 | **Longitude** | Also computed internally in the GPS receiver. [deg] |
| 174 | **Groundspeed** | Computed internally in the GPS receiver (by differentiating the position data with respect to time). [m/s] |
| 175 | **Ground Track Angle** | The direction towards which the aircraft is moving relative to the ground, with respect to magnetic north. [deg] |
| 176 | **Magnetic Deviation** | The difference between magnetic north and true north as indicated automatically by the GPS receiver based on the current position. [deg] |
| 177 | **Time Since Solution** | The time since the GPS was last able to compute an accurate position solution based on a sufficient number of satellites. It updates position based on dead reckoning if it does not have a sufficient number of satellites in view. [s] |
| 178 | **Track Angle Error** | Angle between actual track and desired track between two GPS way points. This is meaningless if no way points have been selected. [deg] |
| 200 | **Date** | As indicated by the data acquisition system computer clock. [yymmdd] |
| 201 | **Month** | mm [integer number] |
| 202 | **Day** | dd [integer number] |
| 203 | **Year** | yy [integer number] |

| | | |
|---|---|---|
| 204 | **Flight** | A serial number assigned to each T-28 flight beginning with the first flight. (Flight #1 occurred in 1972.) |
| 205 | **Altitude** | The altitude in a standard atmosphere corresponding to the recorded pressure. [m] |
| 206 | **Theta e** | The equivalent potential temperature corresponding to the recorded temperature and assuming saturation with respect to liquid water. [K] |
| 207 | **Saturation Mixing Ratio** | The mixing ratio of water vapor corresponding to saturation with respect to liquid water at the recorded temperature. [g/kg] |
| 208 | **Point dz/dt** | The rate of change of altitude of the aircraft computed by differentiating the pressure altitude with respect to time. This represents an independent estimate of the rate of climb to be compared to tag 105. [m/s] |
| 209 | **Indicated Air Speed** | What the airspeed would be if the aircraft were flying at sea level and indicating the observed dynamic pressure. [m/s] |
| 210 | **Updraft (uncorrected)** | The estimated upward speed of the air relative to the ground computed from changes in the aircraft altitude and other factors, but not corrected for horizontal aircraft acceleration. [m/s] |
| 211 | **Calculated TAS** | The true speed of the aircraft relative to the air computed from the observed dynamic and static pressures, and temperature. [m/s] |

| | | |
|---|---|---|
| 212 | **Updraft Correction Factor** | A correction to the simple (uncorrected) updraft calculation that accounts for horizontal accelerations of the aircraft. [m/s] |
| 213 | **Cooper Updraft** | The sum of the uncorrected updraft and the correction factor. [m/s] |
| 214 | **Kopp Updraft** | An updraft calculated somewhat differently than the Cooper updraft. In most situations, it yields a less noisy and more physically plausible updraft result for the T-28. [m/s] |
| 216 | **Turbulence** | The turbulent energy dissipation rate estimated from observed fluctuations in true airspeed. [$cm^{2/3}/s$] |
| 217 | **Air Density** | Computed from the recorded temperature and static pressure. [kilograms per cubic meter] |
| 218 | **JW Mixing Ratio** | The mixing ratio of cloud water per unit mass of dry air based on the JW reading and computed air density. [g/kg] |
| 219 | **FSSP Mixing Ratio** | The mixing ratio of cloud water per unit mass of dry air calculated from the FSSP water concentration. [g/kg] |
| 220 | **Hail Mixing Ratio** | The mixing ratio of hail particles per unit mass of dry air based on the computed hail water and air density. [g/kg] |
| 260 | **Ambient Vert Electric Field** | The component of the ambient electric field that is vertical in the aircraft frame of reference. Positive means a positive test charge would drift upward relative to the aircraft in the field. [kV/m] |

261 **Plane Vert Electric Field** The field due to charge on the aircraft, computed by summing the readings of the top and bottom mill and normalizing based on self-charging tests. Positive means a positive test charge would be repelled away from the aircraft by the field. [kV/m]

262 **Ambient Hor Electric Field** The ambient field oriented perpendicular to the aircraft along the wings, positive meaning a positive test charge would drift to the right in the field. [kV/m]

263 **Plane Hor Electric Field** The field due to charge on the aircraft, computed by summing the wingtip mill readings and normalizing. Positive means a positive charge would be repelled away from the aircraft due to its charge. [kV/m]

264 **Ambient Vert Field (roll cor)** The component of the ambient field that is truly vertical with respect to earth coordinates. [kV/m]

265 **Ambient Hor Field (roll cor)** The component of the ambient field perpendicular to the aircraft path and truly horizontal with respect to earth coordinates. [kV/m]

272 **Latitude (deg)**

273 **Latitude (min)**

274 **Longitude (deg)**

275 **Longitude (min)** GPS coordinates broken into separate degree and minute components.

276 **Ground Track Angle (True N)** The direction of motion relative to the ground with respect to true north, derived from the GPS ground track angle with respect to magnetic north.

## APPENDIX C

Reduced Data Items Computed for COPS, Norman, Okla May-June, 1991 *0

| Tag # | Description | | # Values Output | Units | Method of Computation | Last Mod (if this year) |
|---|---|---|---|---|---|---|
| 101 | Dynamic Pressure #1 | (10 Hz) | 1 | hPa | 6.280525E-3 * Raw + 0.88244 | |
| 102 | Dynamic Pressure #2 | (10 Hz) | 1 | hPa | 5.268222E-3 * Raw - 0.22955 | |
| 103 | Static Pressure #1 | (2 Hz) | 1 | hPa | 1.5809E-2 * Raw + 528.1485 | |
| 104 | Static Pressure #2 | (2 Hz) | 1 | hPa | 1.09617E-2 * Raw + 688.7589 | |
| 105 | Rate of Climb | | 1 | m/s | 5.625E-4 * Raw, for Raw > = 0<br>5.287E-4 * Raw, for Raw < 0 | |
| 106 | Rosemount Temp | | 1 | deg C | mach2 = 5*((1+dyn_pr/stat_pr)**(2/7)-1)<br>divisor = 1 + 0.195 * mach2<br>temp = (1.83105E-3*Raw+243.16)/divisor-273.16 | |
| 107 | Reverse Flow Temp | | 1 | deg C | divisor = 1 + 0.153 * mach2<br>temp = (1.7962E-3*Raw+244.3775)/divisor-273.16 | *3 |
| 108 | Manifold Pressure | | 1 | " Hg | 3.1098E-3 * Raw + 0.159275 | |
| 109 | Acceleration | (10 Hz) | 1 | g's | 6.25E-5 * Raw + 1.0 | *2 |
| 110 | Pitch | (5 Hz) | 1 | deg | -3.05175E-3 * Raw + 50 | |
| 111 | Roll | (5 Hz) | 1 | deg | 3.05175E-3 * Raw - 50 | |
| 112 | J.W. Liquid Water | | 1 | $g/m^3$ | 1.83125E-4 * Raw | |
| 113 | VOR | | 1 | deg | 1.117534E-2 * Raw - 1.155475 | |
| 114 | DME #1 | | 1 | naut mi | 3.03269E-3 * Raw - 0.24536 | |
| 115 | DME #2 | | 1 | naut mi | 3.03269E-3 * Raw - 0.046623 | |
| 116 | Voltage Regulator | | 1 | volts | 1.5258789E-4 * Raw | |
| 117 | Heading | (5 Hz) | 1 | deg | device not hooked up | |
| 118 | NCAR true? air speed | | 1 | m/s | 3.96744E-3 * Raw | |
| 121 | Interior Temp (computer) | | 1 | deg C | 3.05175E-2 * Raw | |
| 130 | Event Code bits | | 1 | flags | bit 0 = 1 --> system running<br>bit 1 = 0 --> in cloud<br>bit 2 = 0 --> foil on<br>bit 3 = 0 --> voice recorder on | |
| 131 | GPS warning codes | | 1 | flags | 11 bit codes | new 1991 |
| 140 | FSSP counts | | 15 | number | Raw | |
| 141 | FSSP total counts | | 1 | number | Sum of tag 140s | |
| 142 | FSSP ave diameter | | 1 | microns | sum of diams / number | |

| | | | | | | | |
|---|---|---|---|---|---|---|---|
| 143 | FSSP concentration | | 1 | $\#/cm^3$ | vol = 0.229 * tas<br>denom = 1 - .55 * activ / 100<br>conc = tot_count / vol / denom | | |
| 144 | FSSP water | | 1 | $g/m^3$ | mass = sum of counts * volumes<br>water = mass/vol/denom*1.E6 | | |
| 146 | Probe Activity | | 1 | ??? | Raw / 10 | | |
| 147 | PMS 2d Shd Or | | 1 | number | Raw | | |
| 150 | Hail counts | | 14 | number | Raw | | |
| 151 | Slow particles | | 1 | number | Raw | | |
| 152 | Hail total counts | | 1 | number | Sum of tag 150s | | |
| 153 | Hail ave diameter | | 1 | cm | sum of diams / number | | |
| 154 | Hail concentration | | 1 | $\#/m^3$ | tot_counts / (.1 * tas) | | |
| 155 | Hail equiv water | | 1 | $g/m^3$ | mass = sum of counts * volumes * 0.9<br>water = mass / vol | | |
| 160 | Top field mill, low res | (20 Hz) | 1 | kV/m | -1.982574E-2 * Raw + 0.026 | Spring 1991 | (*1) |
| 161 | Bottom field mill, low res | (20 Hz) | 1 | kV/m | -1.982574E-2 * Raw + 0.104 | Spring 1991 | (*1) |
| 162 | Left field mill, low res | (20 Hz) | 1 | kV/m | -9.7023E-2 * Raw - 0.5442 | 5/3/91 | (*1) |
| 163 | Right field mill, low res | (20 Hz) | 1 | kV/m | -9.7778E-2 * Raw - 1.9651 | 5/3/91 | (*1) |
| 164 | Top field mill, hi res | (20 Hz) | 1 | kV/m | -3.11585E-4 * Raw + 0.027 | Spring 1991 | (*1) |
| 165 | Bottom field mill, hi res | (20 Hz) | 1 | kV/m | -3.10364E-4 * Raw + 0.04 | Spring 1991 | (*1) |
| 166 | Left field mill, hi res | (20 Hz) | 1 | kV/m | -1.5323E-3 * Raw + 0.1614 | 5/3/91 | (*1) |
| 167 | Right field mill, hi res | (20 Hz) | 1 | kV/m | -1.5361E-3 * Raw + 0.0835 | 5/3/91 | (*1) |
| 172 | GPS latitude | | 1 | deg | degree + (minute + hundredths/100)/60 | new 1991 | |
| 173 | GPS longitude | | 1 | deg | degree + (minute + hundredths/100)/60 | new 1991 | |
| 174 | GPS groundspeed | | 1 | m/s | 1852 / 36000 * Raw | new 1991 | |
| 175 | GPS grnd track angle (mag N) | | 1 | deg | Raw / 10 | new 1991 | |
| 176 | GPS magnetic deviation | | 1 | deg | Raw / 10 (Raw is 32-bits, not 16) | new 1991 | |
| 177 | GPS time since solution | | 1 | s | Raw / 10 | new 1991 | |
| 178 | GPS track angle error | | 1 | deg | Raw / 10 (Raw is 32-bits, not 16) | new 1991 | |
| 200 | Date | | 1 | yymmdd | | | |
| 201 | Month | | 1 | number | | | |
| 202 | Day | | 1 | number | | | |
| 203 | Year | | 1 | 2-dig | | | |
| 204 | Flight number | | 1 | number | | | |
| 205 | Altitude | | 1 | meters | 4.43077E4*(1-(stat_pr/1013.3027)**.190284) | | |

| | | | | | | |
|---|---|---|---|---|---|---|
| 206 | Theta e | 1 | K | tempk = RFT temp in K<br>svp = 6.1078*exp(17.26939*rft/(tempk-35.86))<br>smr = svp / (stat_pr - svp) * 0.622<br>ts = tempk * (1000/stat_pr)**0.286<br>thetae = ts*exp(597.3*smr)/(0.24*tempk)) | | |
| 207 | Saturation mixing ratio | 1 | | smr from above | | |
| 208 | Point dz/dt | 1 | m/s | alt - prev_alt | | |
| 209 | Indicated airspeed | 1 | m/s | c = 1 + dyn_pr / 1013.3027<br>ias=sqrt(5.79E5*(c**(2/7)-1)) | | |
| 210 | Updraft (uncorrected) | 1 | m/s | u1 = change in alt ((i+1)-(i-1))/2<br>u2 = (27 - man_pr) * 92<br>u3 = (1.94254 * ias - 140) * 17.7<br>updr = u1 + (u2 + u3) * 0.00508 | | |
| 211 | Calculated TAS | 1 | m/s | sqrt(rftuc*mach2*401.856/divisor) | | |
| 212 | Updraft correction factor | 1 | m/s | calc_tas*(change in calc_tas)/2/9.775 | | |
| 213 | Cooper Updraft | 1 | m/s | updraft + updraft correction | | |
| 214 | Kopp Updraft | 1 | m/s | dens = 0.34838 * stat_pr /tempk<br>ang = pitch * 0.0174533<br>Kopp=u1+62.12*accel*9.775/(dens*calc_tas)<br>-(0.02028+ang)*calc_tas | | |
| 216 | Turbulence | 1 | $cm^{**2/3}/s$ | Much too complicated to write here.<br>Static and dynamic pressure values,<br>along with RFTs, are fed into a fast Fourier<br>transform routine. Consult program listing. | | |
| 217 | Air density | 1 | $kg/m^3$ | 0.34838 * stat_pr / tempk | | |
| 218 | JW mixing ratio | 1 | g/kg | jw_water / density | | |
| 219 | FSSP mixing ratio | 1 | g/kg | FSSP_water / density | | |
| 220 | Hail mixing ratio | 1 | g/kg | hail_water / density | | |
| 260 | Ambient vert EF | 1 | kV/m | (tfm / 1.9 - bfm) / 5.6 | 5/5/91 | (*1) |
| 261 | Plane vert EF | 1 | kV/m | (tfm / 2 + bfm) / 4 | 5/5/91 | (*1) |
| 262 | Ambient lateral EF | 1 | kV/m | (rfm - lfm) / 44.8 | 5/5/91 | (*1) |
| 263 | Plane lateral EF | 1 | kV/m | (rfm + lfm) / 21.6 | 5/5/91 | (*1) |
| 264 | Ambient vert EF (with roll) | 1 | kV/m | cosr = cos(roll_rad)<br>sinr = sin(roll_rad)<br>t264 = t260 * cosr + t262 * sinr | | (*1) |
| 265 | Ambient lat EF (with roll) | 1 | kV/m | t265 = -t260 * sinr + t262 * cosr | | (*1) |

| | | | | | |
|---|---|---|---|---|---|
| 272 | GPS deg lat | 1 | deg | integer portion of tag 172 (t172) | new 1991 |
| 273 | GPS min lat | 1 | min | fractional part of t172 * 60 | new 1991 |
| 274 | GPS deg long | 1 | deg | integer portion of tag 173 (t173) | new 1991 |
| 275 | GPS min long | 1 | min | fractional part of t173 * 60 | new 1991 |
| 276 | GPS true bearing | 1 | deg | mod(t175+t176+360,360) | new 1991 |

*0 - In some cases the equation variables are averages. Consult the listing of REDUCE.C for exact details. All parameters are recorded at 1 Hz unless otherwise noted.

*1 - The sign convention for field mills was reversed from that used previously. Currently electric field is reported, whereas prior to 1991 potential gradient was reported.

*2 - Accelerometer wasn't working for flights 541-543, so rate of climb or second derivative of altitude was used to calculate acceleration.

*3 - Reverse flow was unreliable. Reduction program was modified after the field season to allow substitution of Rosemount for RFT in equations using temperature.

## APPENDIX D

T-28 COPS-91 Flight Tracks*

*Reference grid is GPS latitude/longitude with Cimarron radar spider web overlaid. Range rings are in kilometers.

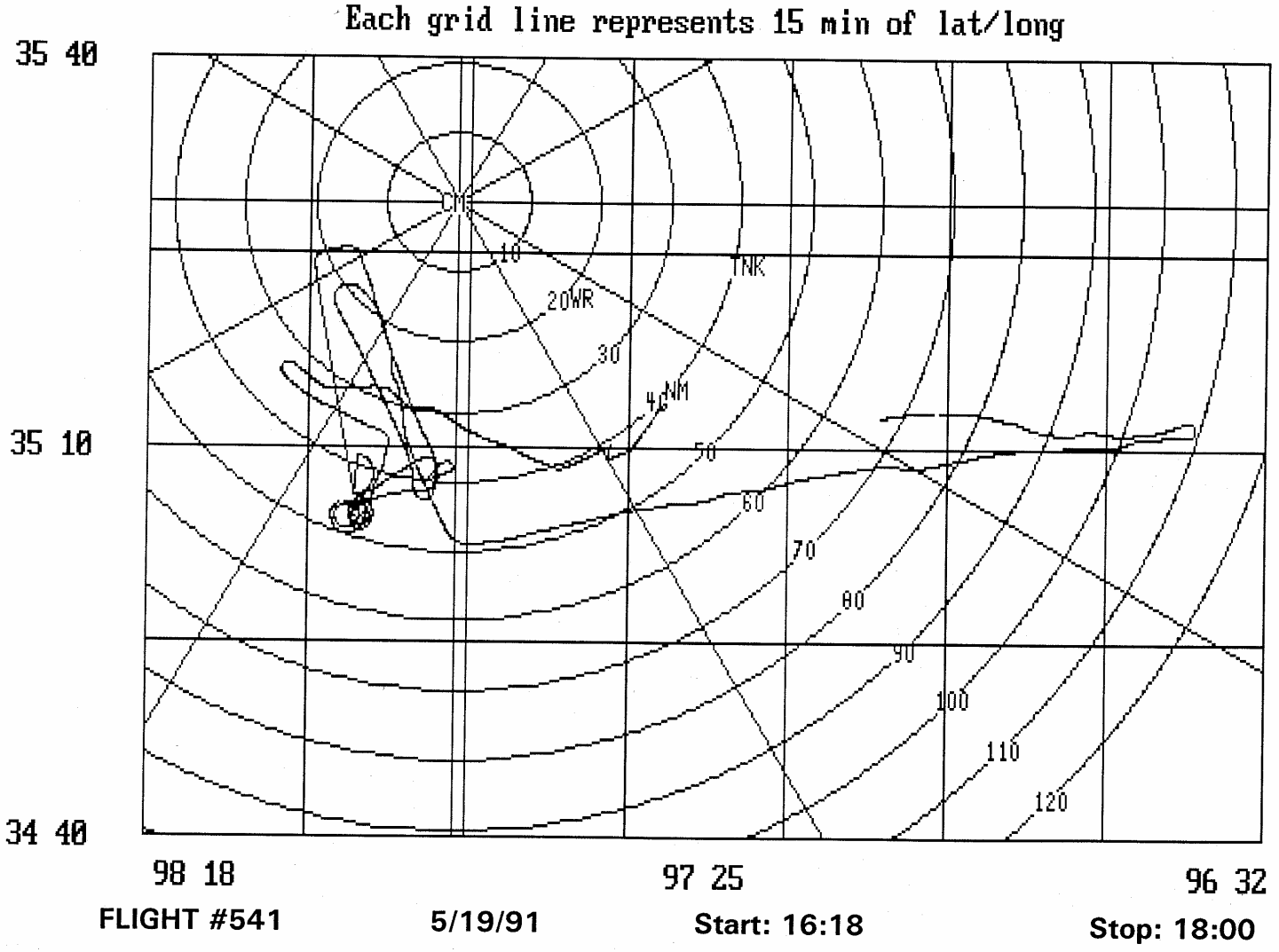
Each grid line represents 15 min of lat/long
35 40
35 10
34 40
98 18
97 25
96 32
CHS
10
20WR
30
40NM
TNK
50
60
70
80
90
100
110
120
FLIGHT #541
5/19/91
Start: 16:18
Stop: 18:00

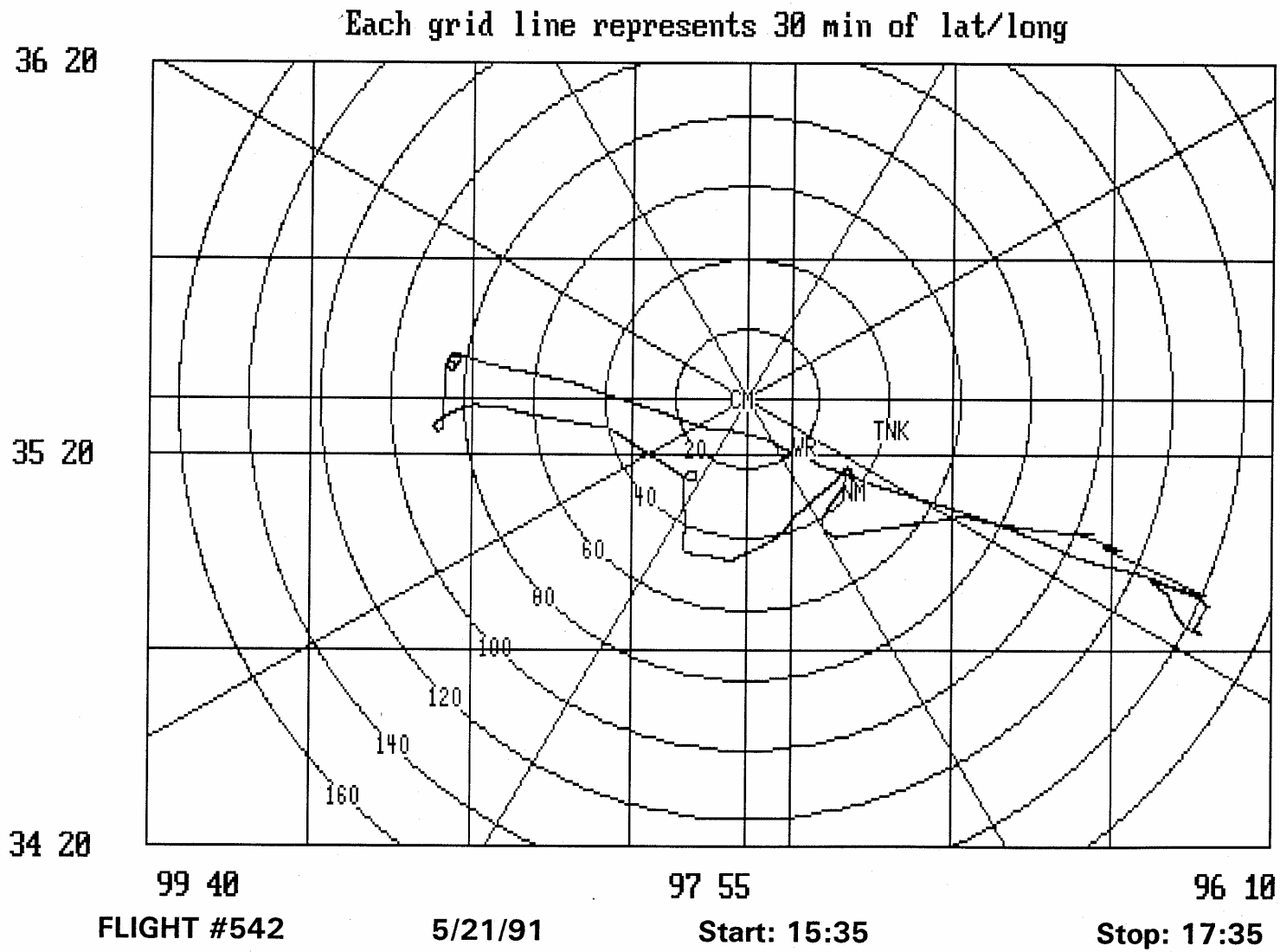
Each grid line represents 30 min of lat/long
36 20
35 20
34 20
99 40
97 55
96 10
CH
TNK
WR
NM
20
40
60
80
100
120
140
160
FLIGHT #542
5/21/91
Start: 15:35
Stop: 17:35

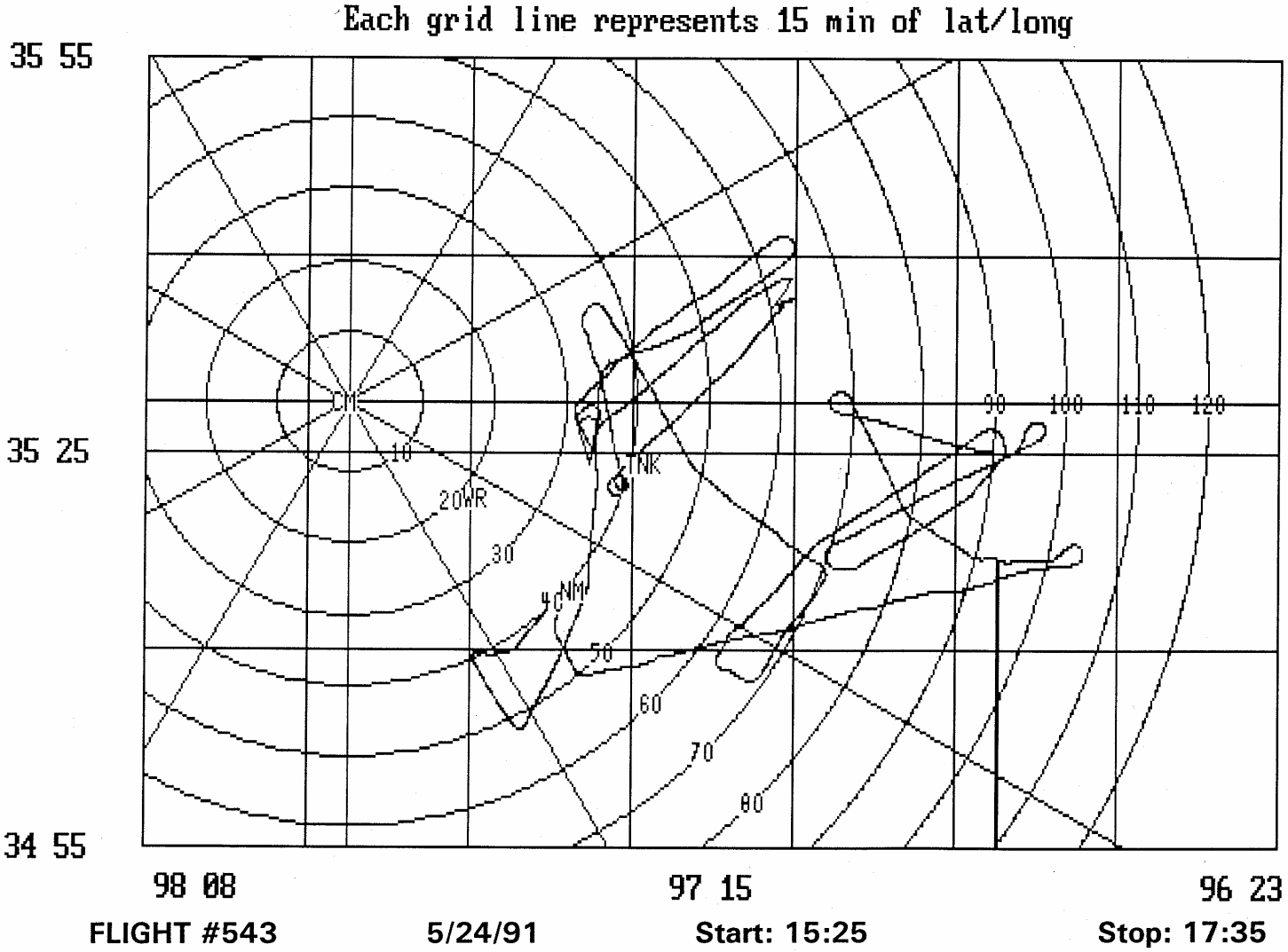
Each grid line represents 15 min of lat/long
35 55
35 25
34 55
98 08
97 15
96 23
CM
TNK
10
20NM
30
40NM
50
60
70
80
90
100
110
120
FLIGHT #543
5/24/91
Start: 15:25
Stop: 17:35

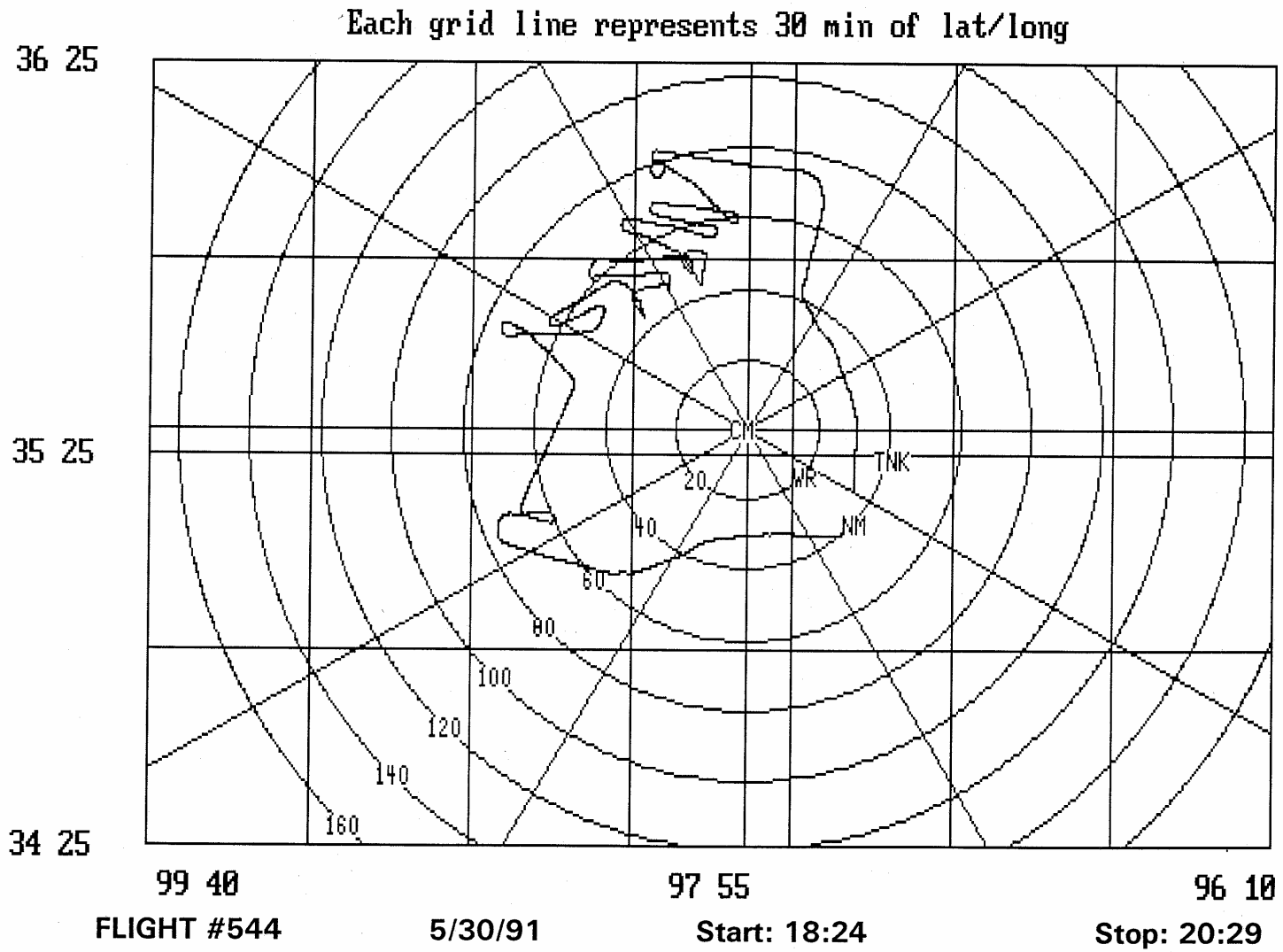
Each grid line represents 30 min of lat/long
36 25
35 25
34 25
99 40
97 55
96 10
CM
TNK
WR
NM
20
40
60
80
100
120
140
160
FLIGHT #544
5/30/91
Start: 18:24
Stop: 20:29

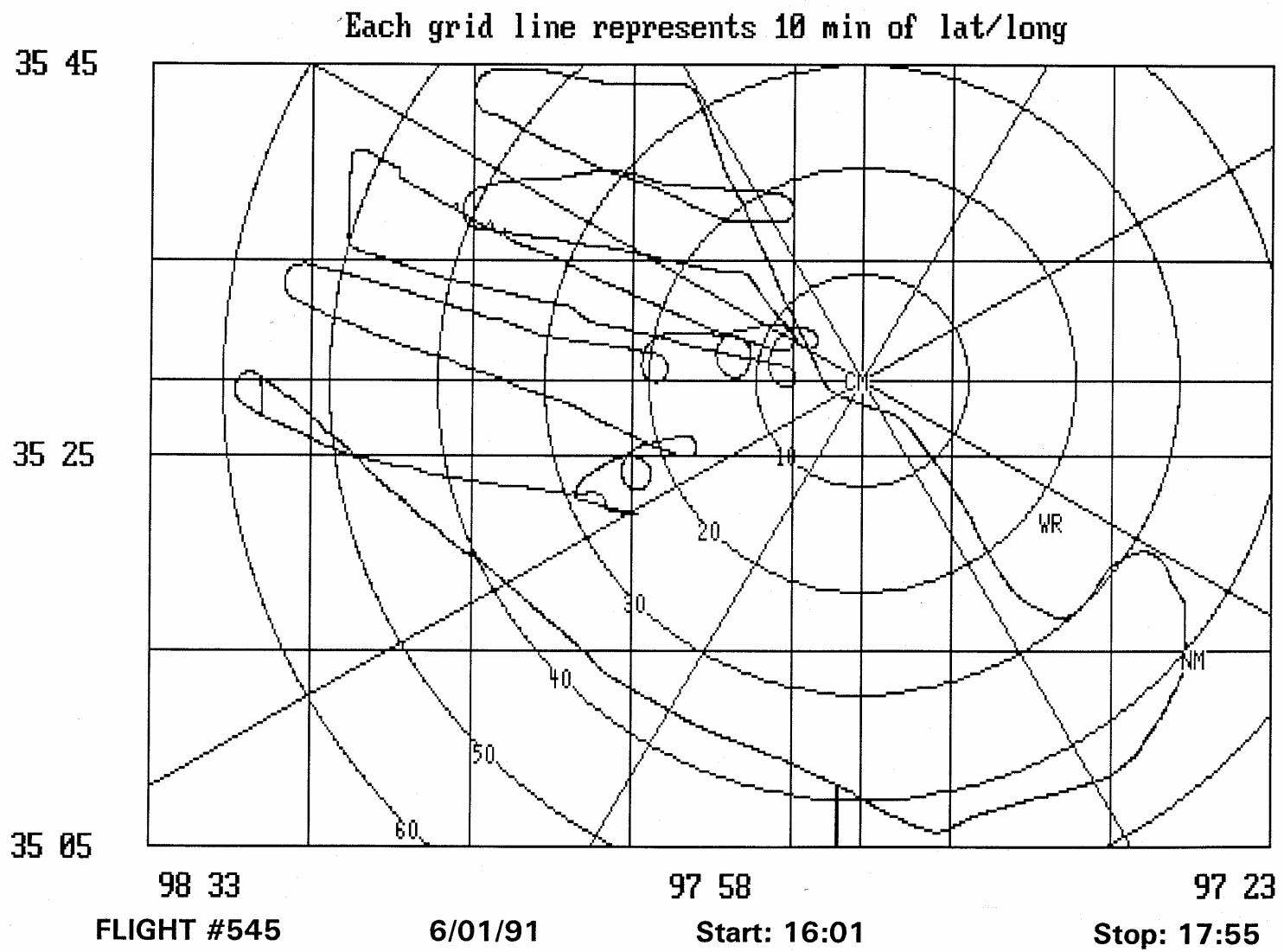
Each grid line represents 10 min of lat/long
35 45
35 25
35 05
98 33
97 58
97 23
CM
WR
NM
10
20
30
40
50
60
FLIGHT #545
6/01/91
Start: 16:01
Stop: 17:55

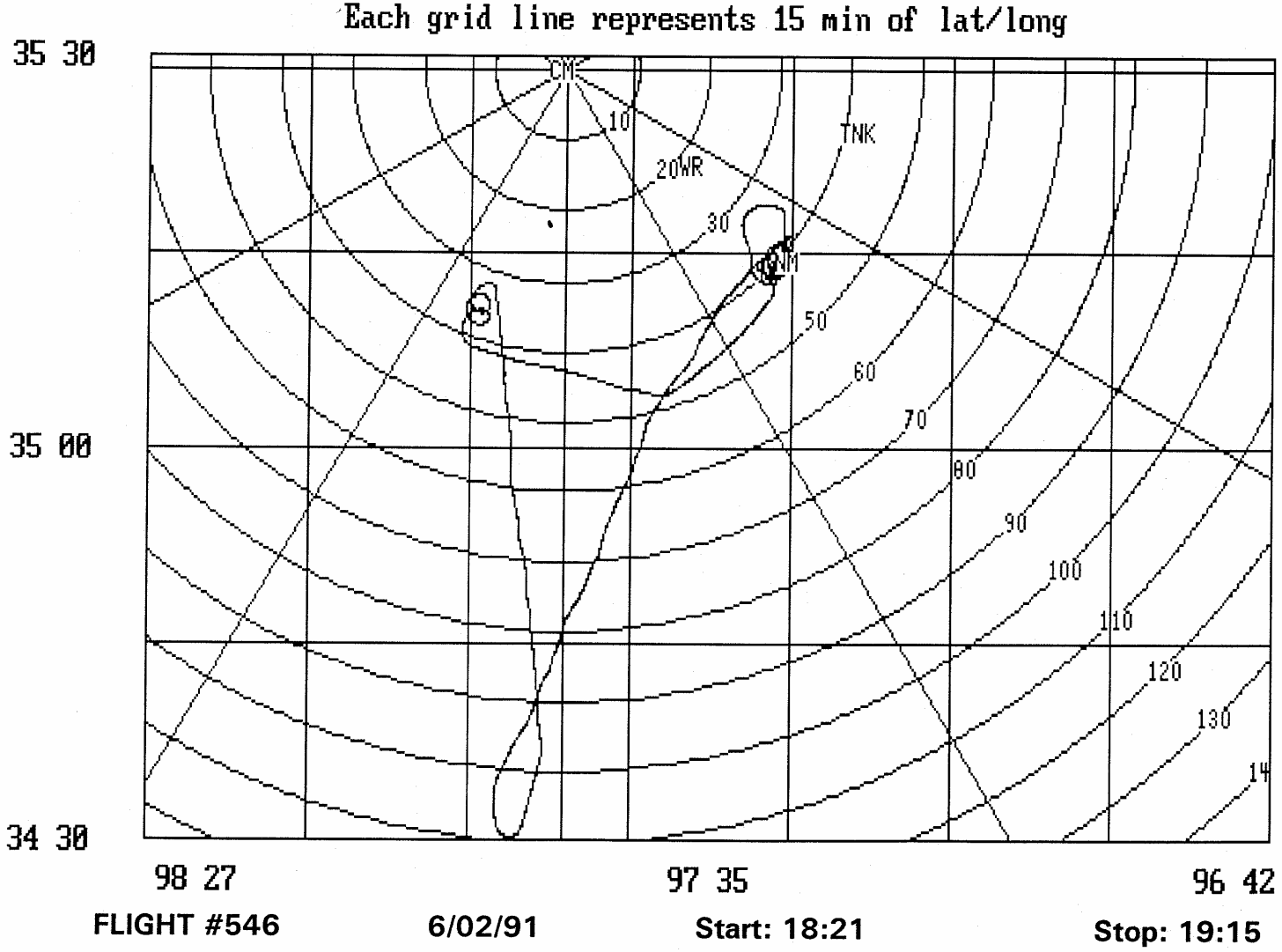
Each grid line represents 15 min of lat/long
35 30
35 00
34 30
98 27
97 35
96 42
CM
10
20WR
30
TNK
50
60
70
80
90
100
110
120
130
14
FLIGHT #546
6/02/91
Start: 18:21
Stop: 19:15

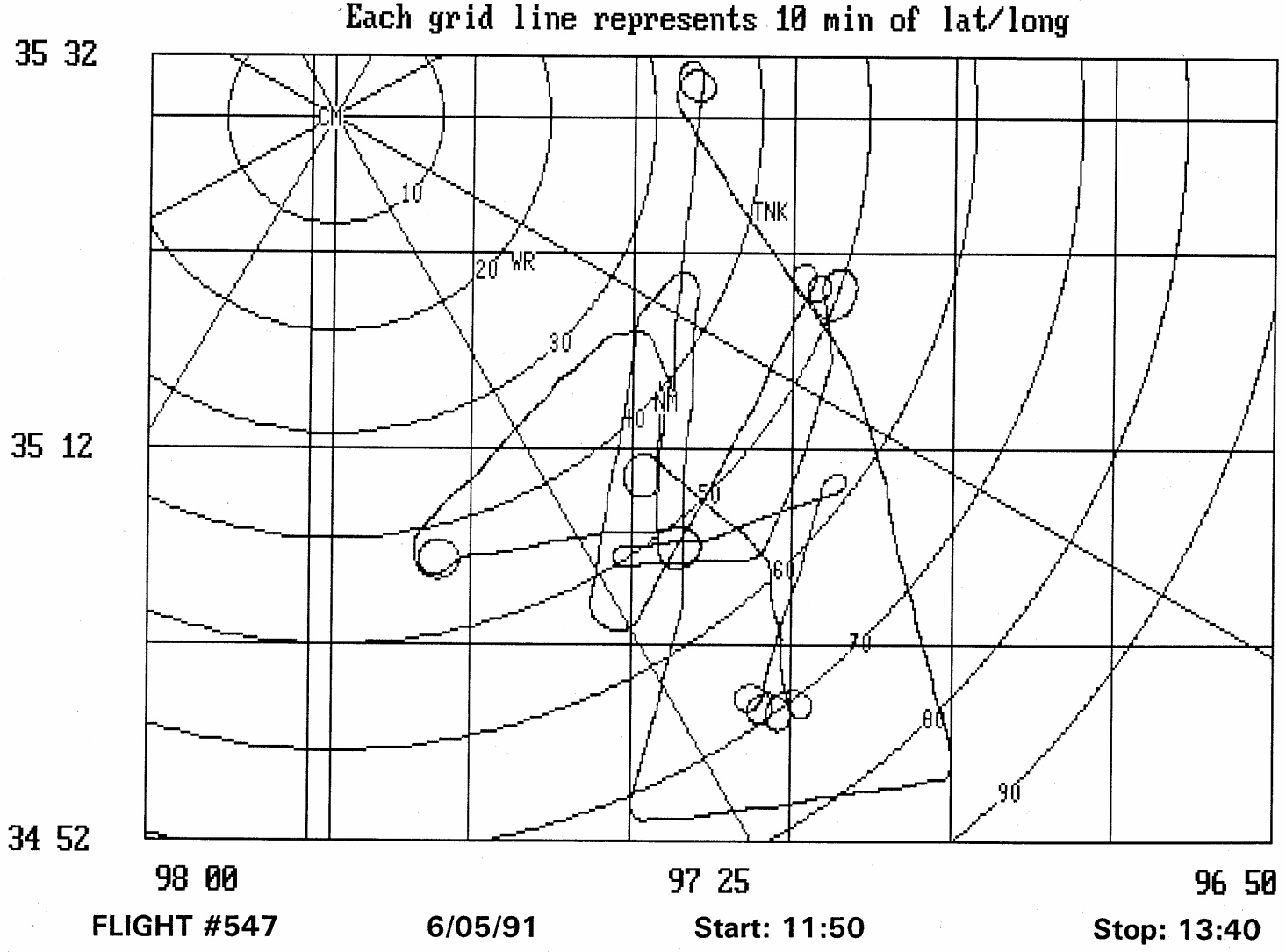
Each grid line represents 10 min of lat/long
35 32
35 12
34 52
98 00
97 25
96 50
CH
10
20
WR
30
TNK
NM
40
50
60
70
80
90
FLIGHT #547
6/05/91
Start: 11:50
Stop: 13:40

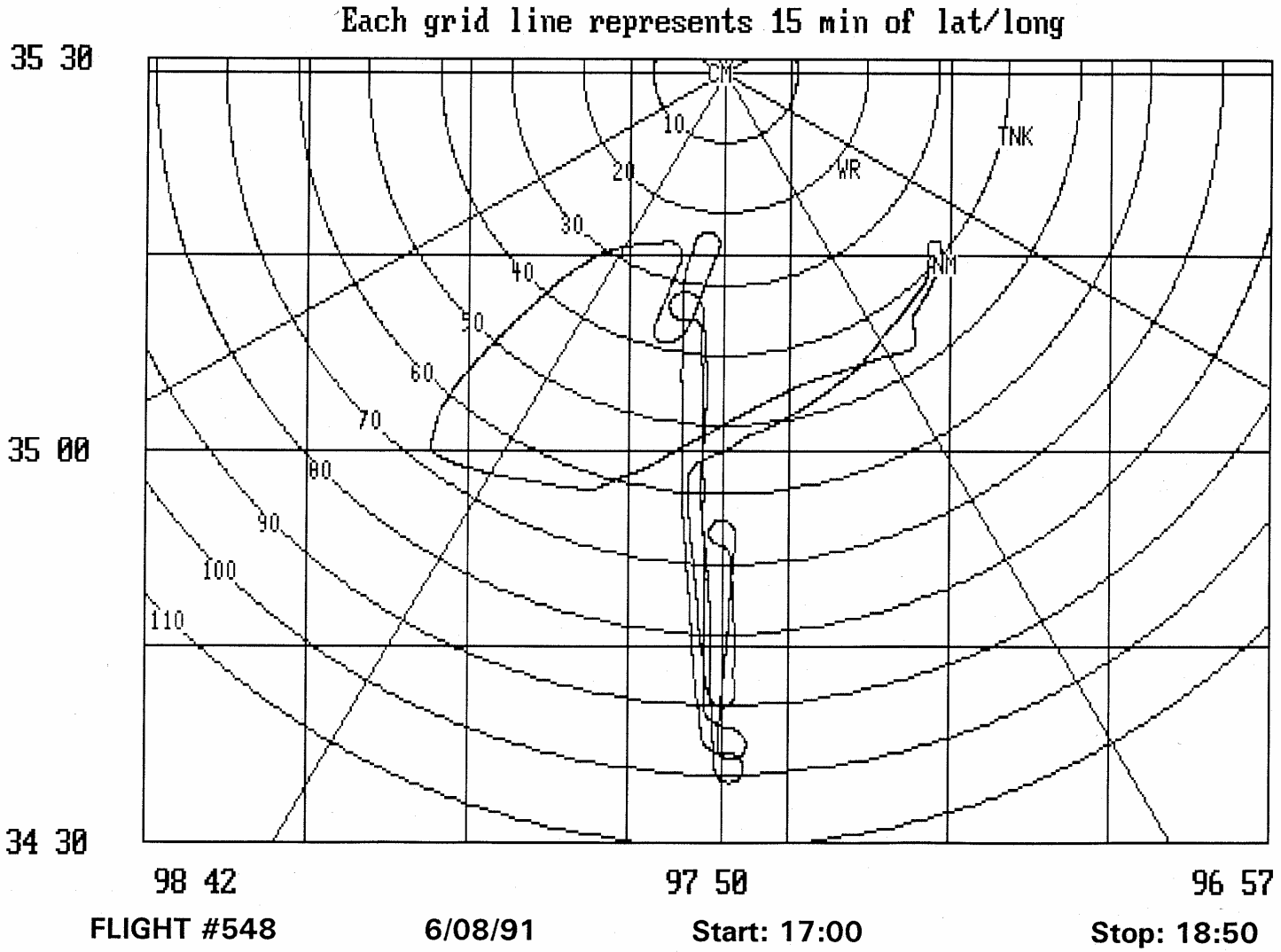
Each grid line represents 15 min of lat/long
35 30
35 00
34 30
98 42
97 50
96 57
CM
WR
TNK
RNM
10
20
30
40
50
60
70
80
90
100
110
FLIGHT #548
6/08/91
Start: 17:00
Stop: 18:50